

© Copyright by

Manki Cho

August, 2014

**STEKLOV EIGENPROBLEMS AND APPROXIMATIONS
OF HARMONIC FUNCTIONS**

A Dissertation

Presented to

the Faculty of the Department of Mathematics

University of Houston

In Partial Fulfillment

of the Requirements for the Degree

Doctor of Philosophy

By

Manki Cho

August, 2014

STEKLOV EIGENPROBLEMS AND APPROXIMATIONS OF HARMONIC FUNCTIONS

Manki Cho

Approved:

Dr. Giles Auchmuty (Committee Chair)
Department of Mathematics, University of Houston

Committee Members:

Dr. Tsorng-Whay Pan
Department of Mathematics, University of Houston

Dr. Daniel Onofrei
Department of Mathematics, University of Houston

Dr. Ralph William Metcalfe
Department of Mechanical Engineering
University of Houston

Dean, College of Natural Sciences and Mathematics
University of Houston

Acknowledgements

I would like to sincerely thank my Ph.D. thesis advisor, Dr. Giles Auchmuty, for his never-ending encouragement, support, inspiration, and patience. Dr. Giles Auchmuty has taught me everything that I know about partial differential equations and he helped me to be a better mathematician. I feel extremely honored to do my research under his guidance. Moreover, I acknowledge him for his concerns about my family. I would never forget his care about my family.

I would also like to express my gratitude to my committee members, Dr. Tsorng-Whay Pan, Dr. Daniel Onofrei, and Dr. Ralph Metcalfe for spending their times to read my thesis carefully and for the valuable comments and suggestions. I am also very thankful to all the academic and administrative members in the Department of Mathematics at the University of Houston. In particular, I would like to thank Dr. Shanyu Ji for his support and care during my graduate years. I would like to thank all my fellow graduate students for sharing and spending their times with me.

I dedicate the thesis to my parents and family. My parents, Sungoh Cho and Myoeung Kim and my younger brother, Youngki Cho have always loved, encouraged, and supported me. There is no word that I could describe my love to my lovely wife, Mikyoung Park. Without her, this work could never have been done. Special thanks go to my adorable babies, Yena Cho and Mason Yongjae Cho for their love and smiles.

**STEKLOV EIGENPROBLEMS AND APPROXIMATIONS
OF HARMONIC FUNCTIONS**

An Abstract of a Dissertation

Presented to

the Faculty of the Department of Mathematics

University of Houston

In Partial Fulfillment

of the Requirements for the Degree

Doctor of Philosophy

By

Manki Cho

August, 2014

Abstract

In this work, we provide explicit formulae for harmonic Steklov eigenvalues and associated Steklov eigenfunctions by solving a Steklov eigenproblem on bounded rectangles in \mathbb{R}^2 . This allows the description of all the Steklov eigenvalues and their corresponding Steklov eigenfunctions.

The harmonic Steklov eigenfunctions provide orthogonal sets in $H^1(\Omega)$ and complete orthonormal bases of $L^2(\partial\Omega, d\sigma)$. This enables us to study Steklov eigenfunction expansions of harmonic functions. Comparing against the expansion in terms of Neumann eigenfunctions, the Steklov expansions usually converge faster than the Neumann expansions. Results are described by relative errors of finite terms of each expansion with respect to the L^2 , L^∞ , and gradient norms.

Solutions of Laplace's equation subject to inhomogeneous Dirichlet, Neumann, Robin, or other boundary data are approximated by Steklov expansions. These representations involve boundary conditions and explicit spectral approximations are found.

In the end, we provide the general formulae for $u(0,0)$ where harmonic functions $u(x,y)$ are solutions of boundary value problems on a rectangle. These harmonic functions are determined precisely in terms of their respective boundary data.

Contents

Abstract	v
1 Introduction	1
2 Assumptions, Definitions, and Notations	4
3 Harmonic Steklov Eigenvalues and Eigenfunctions	7
3.1 Analytic Solutions of the Steklov Eigenproblem	7
3.2 Families of Steklov Eigenfunctions	9
3.3 The Determining Equations	16
3.4 A Special Solution	20
3.5 The Ordering of Eigenfunctions and Eigenvalues	21
3.6 Normalized Steklov Eigenfunctions	25
4 Spectral Representations for Harmonic Functions	32
4.1 The Steklov Expansion	32
4.2 Relative Errors for the Steklov Expansion	35
5 Solutions of Boundary Value Problems on Ω	47
5.1 The Harmonic Dirichlet Problem	47

5.2	The Harmonic Neumann Problem	56
5.3	The Harmonic Robin Problem	60
5.4	The Generalized Boundary Data	67
6	An Application of the Steklov Expansion	69
6.1	The Mean Value Property	69
6.2	The Correction Term	74
6.3	Several Examples	76
	Bibliography	82

Chapter 1

Introduction

In this thesis, we mainly study harmonic functions that are solutions of Laplace's equation on bounded regions in \mathbb{R}^2 . Combined with boundary data which may be of Dirichlet, Neumann, or Robin type, there are many questions how harmonic functions can be determined by their respective boundary conditions. Eigenvalue analyses have been studied to provide spectral representations. In Section 9 and 10 of [1], applications and some results of Steklov eigenproblems for prototypical second order elliptic partial differential operators on the regions in \mathbb{R}^2 were described. For these eigenproblems, the existence of an infinite and discrete spectrum is demonstrated.

We begin in Chapter 3 with a Steklov eigenproblem on bounded rectangle $\Omega = [-L, L] \times [-Lh, Lh]$ for non zero constants L and h . The first positive eigenvalue and a corresponding eigenfunction of this problem may be found by variational principles. The description is developed in Section 3 of [1] and a different variational principle is described in Chapter 3 of [6]. Separation of variables of $(x, y) \in \mathbb{R}^2$ will be used to provide explicit formulae for all Steklov eigenvalues and corresponding Steklov eigenfunctions. Determining equations will be derived from the boundary condition

and their solutions are involved in Steklov eigenvalues and eigenfunctions.

Families of Steklov eigenfunctions are described and classified by their boundary functions. The maximal orthonormal set in $L^2(\partial\Omega, d\sigma)$ will be constructed by the boundary values of Steklov eigenfunctions. Also Steklov eigenfunctions provide an orthogonal basis of the space of all harmonic functions on Ω with respect to a special inner product. These results lead to orthogonal series expansion, in terms of the Steklov eigenfunctions, for harmonic functions. The approximations depend only on the boundary values. This series converges strongly in $H^1(\Omega)$ with respect to the ∂ -inner product.

In Chapter 4 the Neumann eigenproblem is introduced and eigenfunctions of this problem will be normalized with respect to $L^2(\Omega)$. The Steklov expansion will be compared against the Neumann expansion, defined by the set of Neumann eigenfunctions, for harmonic functions. Numerical experiments support that the M -th partial sum of the Steklov expansion converges faster than the Neumann one.

These results will be used to describe Steklov spectral representation of solutions of Laplace's equation with non homogeneous boundary conditions. Dirichlet, Neumann and Robin type boundary conditions are considered and generalized in Chapter 5. Results about completeness of these representations rely on that the set of Steklov eigenfunctions may provide an orthonormal basis of $L^2(\partial\Omega, d\sigma)$ and also an orthogonal basis of the space of harmonic functions on Ω .

An approximated solution defined by the finite partial sum of series expansion will be used to describe the unique solution of boundary valued problems. For each problem, numerical experiments will be implemented and support the description of solutions in $\bar{\Omega}$. Harmonic functions which have complicated boundary functions are considered and experiments implies that only a few terms are required to obtain

pointwise approximations of the solutions.

In Chapter 6 we study correction terms for the *mean value property* of harmonic functions. This yields approximations of $u(0, 0)$ in a certain boundary value problem. Finally we show that the Steklov expansion provides other general formulae for $u(0, 0)$ where $u(x, y)$ are solutions of Laplace's equation with non zero boundary conditions.

Chapter 2

Assumptions, Definitions, and Notations

In this dissertation, a region Ω is a rectangle in \mathbb{R}^2 . The closure of a region is denoted $\bar{\Omega}$ and its boundary is $\partial\Omega := \bar{\Omega} \setminus \Omega$. We shall assume that Ω is bounded in \mathbb{R}^2 and $\partial\Omega$ is compact and Lipschitz.

Here $d\sigma$ will represent Hausdorff one-dimensional measure of arc-length and ν is the outward unit normal at points of $\partial\Omega$. All functions in this work will take value in $[-\infty, \infty]$.

Let $p \in [1, \infty]$ then the real Lebesgue spaces $L^p(\Omega)$ and $L^p(\partial\Omega, d\sigma)$ are defined in the standard manner with their usual p-norm denoted by $\|u\|_p$ and $\|u\|_{p, \partial\Omega}$, respectively. In addition, for the case when $p = 2$, $L^2(\Omega)$ and $L^2(\partial\Omega)$ are real Hilbert spaces with respect to their respective inner products

$$\langle u, v \rangle_{2, \Omega} := \int_{\Omega} u(x)v(x) dx \quad \text{and} \quad \langle u, v \rangle_{2, \partial\Omega} := \int_{\partial\Omega} uv d\sigma \quad (2.1)$$

Here $\int_{\partial\Omega} uv \, d\sigma = \frac{1}{|\partial\Omega|} \int_{\partial\Omega} uv \, d\sigma$ where $|\partial\Omega|$ is the perimeter of the boundary. Denote the mean value of a function u on the boundary by $\bar{u} := \int_{\partial\Omega} u \, d\sigma$.

$W^{1,p}(\Omega)$ denotes the standard Sobolev space of functions on Ω that are in $L^p(\Omega)$ and whose weak derivatives D_1u and D_2u are in $L^2(\Omega)$. It is a real Banach space under the standard $W^{1,p}$ -norm

$$\|u\|_{W^{1,p}(\Omega)} := \left(\int_{\Omega} |u|^p + |\nabla u|^p dx \right)^{\frac{1}{p}} \quad (2.2)$$

where ∇u is the gradient of the function u .

We mainly use the space $H^1(\Omega)$ that is the usual real Sobolev space of functions on Ω corresponding to $W^{1,2}(\Omega)$. It is a real Hilbert space under the standard H^1 -inner product

$$[u, v]_1 = \int_{\Omega} [u(x) \cdot v(x) + \nabla u(x) \cdot \nabla v(x)] dx \quad (2.3)$$

and the associated norm is denoted by $\|u\|_{1,2}$.

The trace of a continuous function on $\bar{\Omega}$ to the boundary $\partial\Omega$ is its restriction to $\partial\Omega$. The trace map of $H^1(\Omega)$ to a class of functions on $\partial\Omega$ is the linear extension of the map restricting Lipschitz continuous functions on $\bar{\Omega}$ to $\partial\Omega$. The region Ω is said to satisfy a *compact trace theorem* provided that the trace mapping $\Gamma : H^1(\Omega) \rightarrow L^2(\partial\Omega, d\sigma)$ is compact (see Chapter 2 of [17]). Sometimes u will be used in place of Γu when considering the trace of a function on $\partial\Omega$. These results are for general u . When $u \in W^{1,1}(\Omega)$, the trace of u on $\partial\Omega$ is well-defined. Also it is a Lebesgue integrable function with respect to σ , more details may be found in Section 4.2 of [16].

Evans and Gariepy (see p133, Theorem 1 of [16]) show that Γ is continuous, and Grisvard (see Theorem 1.5.1.10 of [11]) proves an inequality that implies this compact trace result. Also, DiBenedetto (see Chapter ix, Section 18 of [8]) provides result of

this type.

The region Ω considered in this work satisfies the *compact trace theorem*.

Instead of (2.3), we will mainly use the ∂ -inner product

$$[u, v]_{\partial} := \int_{\Omega} \nabla u \cdot \nabla v \, dx + \int_{\partial\Omega} uv \, d\sigma \quad (2.4)$$

The corresponding norm is denoted by $\|u\|_{\partial}$. From Corollary 6.2 of [1], this norm is equivalent to the standard norm of $H^1(\Omega)$. And this is part of Theorem 21A of [21].

A function $u \in H^1(\Omega)$ is said to be *harmonic* on Ω if it satisfies

$$\int_{\Omega} \nabla u \cdot \nabla v \, dx = 0 \quad \text{for all } v \in C_c^1(\Omega) \quad (2.5)$$

where $C_c^1(\Omega)$ is the set of all C^1 -functions on Ω with compact support in Ω .

$\mathcal{H}(\Omega)$ is defined to be the space of all harmonic functions on Ω . Then the usual Sobolev space $H_0^1(\Omega)$ is the closure of $C_c^1(\Omega)$ in $H^1(\Omega)$ -norm. It is easy to see that $\mathcal{H}(\Omega)$ is ∂ -orthogonal to $H_0^1(\Omega)$ also $H^1(\Omega)$ may be expressed as

$$H^1(\Omega) = H_0^1(\Omega) \oplus_{\partial} \mathcal{H}(\Omega) \quad (2.6)$$

Here \oplus_{∂} represents a ∂ -orthogonal decomposition. Zeidler provides the discussion about this result in Section 22.4 of [21].

In this work, we will use the letter e to specify a power-of-ten scale factor. All boundary and area integrals in thesis are computed approximately on Matlab(see [12]) by using adaptive Simpson's method(see Chapter 6 of [7]) with a tolerance, e^{-6} .

Chapter 3

Harmonic Steklov Eigenvalues and Eigenfunctions

3.1 Analytic Solutions of the Steklov Eigenproblem

Let Ω be the two-dimensional rectangle $[-L, L] \times [-Lh, Lh]$ in the xy -plane for positive constants L and h . Here h is called the *aspect ratio*. Denote the boundary segments by Γ_1 for $y = -Lh$, Γ_2 for $x = L$, Γ_3 for $y = Lh$, and Γ_4 for $x = -L$ (see Figure (3.1)).

Consider the problem of finding non trivial functions $s(x, y) \in H^1(\Omega)$ and the real values δ that satisfy

$$\Delta s = 0 \quad \text{in } \Omega \tag{3.1}$$

$$D_\nu s = \delta s \quad \text{on } \partial\Omega \tag{3.2}$$

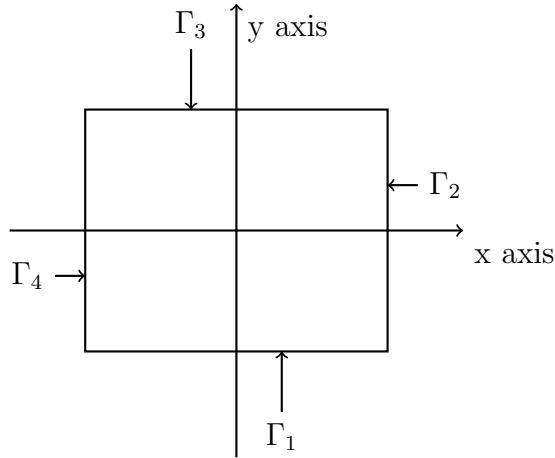


Figure 3.1: The boundary segments of Ω

Here Δ is the Laplacian and $D_\nu s$ is the unit outward normal derivative of s on the boundary. A non-zero function $s(x, y) \in H^1(\Omega)$ is said to be a *harmonic Steklov eigenfunction* on Ω corresponding to the harmonic Steklov eigenvalue δ .

The weak form of (3.1)-(3.2) is to find (δ, s) in $\mathbb{R} \times H^1(\Omega)$ satisfying

$$\int_{\Omega} \nabla s \cdot \nabla v \, dx = \delta \int_{\partial\Omega} sv \, d\sigma \quad \text{for all } v \in H^1(\Omega) \quad (3.3)$$

This harmonic Steklov eigenproblem has been studied for a long time, particularly as it has been treated for the sloshing of a perfect fluid in a tank (see Fox and Kutter [10] or McIver [18]).

$\delta_0 = 0$ is the least Steklov eigenvalue of this problem corresponding to the eigenfunction $s_0(x, y) \equiv 1$ on Ω . This eigenvalue is simple. By setting $s = v$ in (3.3) we see that all other Steklov eigenvalues are positive. An efficient computational approach to obtaining the Steklov eigenvalues and eigenfunctions via a generalized eigenvalue formulation is developed in [14]. Here we shall find all strictly positive

3.2 FAMILIES OF STEKLOV EIGENFUNCTIONS

Steklov eigenvalues and associated Steklov eigenfunctions.

Assume that

$$s(x, y) = V(x)W(y) \quad (3.4)$$

Substituting (3.4) into (3.1) yields

$$V''W + VW'' = 0 \quad \text{on } \Omega \quad (3.5)$$

Or dividing by VW

$$-\frac{V''}{V} = \frac{W''}{W} = b \quad (3.6)$$

Here b is a constant and we obtain two ordinary differential equations for $V(x)$ and $W(y)$

$$V'' = -bV \quad \text{and} \quad W'' = bW \quad \text{on } \Omega \quad (3.7)$$

There are four classes of eigenfunctions for constants θ_1 , θ_2 , and $b := \pm\nu^2$ given by

$$\left\{ \begin{array}{l} \text{(I).} \quad s(x, y) = \sin(\nu x + \theta_1) \sinh(\nu y + \theta_2) \\ \text{(II).} \quad s(x, y) = \sinh(\nu x + \theta_1) \sin(\nu y + \theta_2) \\ \text{(III).} \quad s(x, y) = \cos(\nu x + \theta_1) \cosh(\nu y + \theta_2) \\ \text{(IV).} \quad s(x, y) = \cosh(\nu x + \theta_1) \cos(\nu y + \theta_2) \end{array} \right.$$

3.2 Families of Steklov Eigenfunctions

For each family of eigenfunctions, there are respective conditions on ν for the solutions to obey the boundary conditions. Consider $s(x, y) = \sin(\nu x + \theta_1) \sinh(\nu y + \theta_2)$. Without loss of generality, we can assume $\nu \geq 0$. If $\nu = 0$ then $s(x, y) = \text{constant}$ and

3.2 FAMILIES OF STEKLOV EIGENFUNCTIONS

$\delta = 0$.

For these families of eigenfunctions, the boundary condition at $x = -L$ is that

$$-\frac{\partial s}{\partial x}(-L, y) = \delta s(L, y) \quad (3.8)$$

This becomes, for the family (I) of eigenfunctions

$$-\nu \cos(-\nu L + \theta_1) \sinh(\nu y + \theta_2) = \delta \sin(-\nu L + \theta_1) \sinh(\nu y + \theta_2) \quad (3.9)$$

Then we obtain an equation for the Steklov eigenvalues,

$$\delta = -\nu \cot(-\nu L + \theta_1). \quad (3.10)$$

And the boundary condition at $x = L$ is that,

$$\frac{\partial s}{\partial x}(L, y) = \delta s(L, y) \quad (3.11)$$

This provides a different equation for δ ,

$$\delta = \nu \cot(\nu L + \theta_1) \quad (3.12)$$

Combining (3.10) and (3.12) yields

$$\nu[\cot(-\nu L + \theta_1) + \cot(\nu L + \theta_1)] = 0 \quad (3.13)$$

3.2 FAMILIES OF STEKLOV EIGENFUNCTIONS

Since $\nu > 0$, $\cot(-\nu L + \theta_1) + \cot(\nu L + \theta_1) = 0$ or

$$\frac{\cos(-\nu L + \theta_1)}{\sin(-\nu L + \theta_1)} + \frac{\cos(\nu L + \theta_1)}{\sin(\nu L + \theta_1)} = 0 \quad (3.14)$$

It is equivalent to

$$\cos(-\nu L + \theta_1) \sin(\nu L + \theta_1) + \cos(\nu L + \theta_1) \sin(-\nu L + \theta_1) = 0 \quad (3.15)$$

This implies $\sin(2\theta_1) = 0$, hence $\theta_1 = \frac{k\pi}{2}$, for $k \in \{0, 1, 2, \dots\}$. Substitute it, then

$$s_k(x, y) = \sin\left(\nu x + \frac{k\pi}{2}\right) \sinh(\nu y + \theta_2) \quad (3.16)$$

$$\delta_k = \nu \cot\left(\nu L + \frac{k\pi}{2}\right) \quad (3.17)$$

If k is even then $\sin\left(\nu x + \frac{k\pi}{2}\right) = \pm \sin(\nu x)$. If k is odd then $\sin\left(\nu x + \frac{k\pi}{2}\right) = \mp \cos(\nu x)$.

Now, we shall consider the boundary conditions on Γ_1 and Γ_3 . The boundary condition at $y = -Lh$,

$$-\frac{\partial s}{\partial y}(x, -Lh) = \delta s(x, -Lh) \quad (3.18)$$

implies that

$$-\nu \sin\left(\nu x + \frac{k\pi}{2}\right) \cosh(-\nu Lh + \theta_2) = \delta \sin\left(\nu x + \frac{k\pi}{2}\right) \sinh(-\nu Lh + \theta_2) \quad (3.19)$$

Equation (3.19) becomes

$$\delta = -\nu \coth(-\nu Lh + \theta_2) \quad (3.20)$$

3.2 FAMILIES OF STEKLOV EIGENFUNCTIONS

Similarly, the boundary condition on Γ_3 ,

$$\frac{\partial s}{\partial y}(x, Lh) = \delta s(x, Lh) \quad (3.21)$$

yields that

$$\delta = \nu \coth(\nu Lh + \theta_2) \quad (3.22)$$

We combine (3.20) and (3.22) to have

$$\nu[\coth(-\nu Lh + \theta_2) + \coth(\nu Lh + \theta_2)] = 0 \quad (3.23)$$

When $\nu \neq 0$, then

$$\frac{\cosh(-\nu Lh + \theta_2)}{\sinh(-\nu Lh + \theta_2)} + \frac{\cosh(\nu Lh + \theta_2)}{\sinh(\nu Lh + \theta_2)} = 0 \quad (3.24)$$

Then we see that $\sinh(2\theta_2) = 0$, so $\theta_2 = 0$. Finally, we arrive at

$$s_k(x, y) = \sin(\nu x) \sinh(\nu y) \quad \text{if } k \text{ is even} \quad (3.25)$$

$$\text{or } s_k(x, y) = \cos(\nu x) \sinh(\nu y) \quad \text{if } k \text{ is odd} \quad (3.26)$$

$$\delta = \nu \coth(\nu Lh) \quad (3.27)$$

On the other hand, so far we found two different equations of ν for δ , (3.17) and (3.27). Combining them provides $\nu = 0$ or else

$$\coth(\nu Lh) - \cot(\nu L + \frac{k\pi}{2}) = 0 \quad (3.28)$$

If k is even, then $\coth(\nu Lh) - \cot(\nu L) = 0$. If k is odd, then $\coth(\nu Lh) + \tan(\nu L) = 0$.

3.2 FAMILIES OF STEKLOV EIGENFUNCTIONS

This will be called the *determining equation*. The left hand side of this equation is denoted by $D(\nu)$. Here we shall provide formulae of all Steklov eigenvalue and corresponding Steklov eigenfunctions together with the determining equations. We list the followings eigenfunctions $s^{(I)}(x, y)$, eigenvalues $\delta_k^{(I)}$, and $\nu_k^{(I)}$ with $D_k^{(I)}(\nu)$ corresponding to $k \pmod{2}$ for the first family (I).

$$\begin{aligned} \text{When } k \equiv 0 \pmod{2}, \quad & s_{2k}^{(I)}(x, y) = \sin(\nu_k^{(I)}x) \sinh(\nu_k^{(I)}y) \\ & \delta_{2k}^{(I)} = \nu_k^{(I)} \cot(\nu_k^{(I)}L) \\ & \nu_k^{(I)} \text{ is the } k\text{-th solution of } D_0^{(I)}(\nu) = 0 \\ & \text{with } D_0^{(I)}(\nu) := \coth(\nu Lh) - \cot(\nu L) \end{aligned}$$

$$\begin{aligned} \text{When } k \equiv 1 \pmod{2}, \quad & s_{2k+1}^{(I)}(x, y) = \cos(\nu_k^{(I)}x) \sinh(\nu_k^{(I)}y) \\ & \delta_{2k+1}^{(I)} = -\nu_k^{(I)} \tan(\nu_k^{(I)}L) \\ & \nu_k^{(I)} \text{ is the } k\text{-th solution of } D_1^{(I)}(\nu) = 0 \\ & \text{with } D_1^{(I)}(\nu) := \coth(\nu Lh) + \tan(\nu L) \end{aligned}$$

For the second group of Steklov eigenfunctions, we may list eigenfunctions $s^{(II)}(x, y)$, eigenvalues $\delta_k^{(II)}$, and $\nu_k^{(II)}$ with $D_k^{(II)}(\nu)$, derived in the same way as for group (I).

$$\begin{aligned} \text{When } k \equiv 0 \pmod{2}, \quad & s_{2k}^{(II)}(x, y) = \sinh(\nu_k^{(II)}x) \sin(\nu_k^{(II)}y) \\ & \delta_{2k}^{(II)} = \nu_k^{(II)} \cot(\nu_k^{(II)}Lh) \\ & \nu_k^{(II)} \text{ is the } k\text{-th solution of } D_0^{(II)}(\nu) = 0 \\ & \text{with } D_0^{(II)}(\nu) := \coth(\nu L) - \cot(\nu Lh) \end{aligned}$$

3.2 FAMILIES OF STEKLOV EIGENFUNCTIONS

When $k \equiv 1 \pmod{2}$,

$$s_{2k+1}^{(II)}(x, y) = \sinh(\nu_k^{(II)}x) \cos(\nu_k^{(II)}y)$$

$$\delta_{2k+1}^{(II)} = -\nu_k^{(II)} \tan(\nu_k^{(II)}Lh)$$

$\nu_k^{(II)}$ is the k -th solution of $D_1^{(II)}(\nu) = 0$

with $D_1^{(II)}(\nu) := \coth(\nu L) + \tan(\nu Lh)$

Next we apply the boundary conditions to Steklov eigenfunction groups (III) and (IV). Consider the group (III), $s(x, y) = \cos(\nu x + \theta_1) \cosh(\nu y + \theta_2)$. The boundary condition on Γ_1 , (3.8) yields

$$\nu \sin(-\nu L + \theta_1) \cosh(\nu y + \theta_2) = \delta \cos(-\nu L + \theta_1) \cosh(\nu y + \theta_2) \quad (3.29)$$

which becomes

$$\delta = \nu \tan(-\nu L + \theta_1) \quad (3.30)$$

Applying (3.11) implies

$$-\nu \sin(\nu L + \theta_1) \cosh(\nu y + \theta_2) = \delta \cos(\nu L + \theta_1) \cosh(\nu y + \theta_2) \quad (3.31)$$

It follows

$$\delta = -\nu \tan(\nu L + \theta_1) \quad (3.32)$$

Then, from (3.30) and (3.32) we obtain an equation of ν

$$\nu[\tan(-\nu L + \theta_1) + \tan(\nu L + \theta_1)] = 0 \quad (3.33)$$

3.2 FAMILIES OF STEKLOV EIGENFUNCTIONS

Hence we see that $\sin(2\theta_1) = 0$. Again $\theta_1 = \frac{k\pi}{2}$, for $k \in \{0, 1, 2, \dots\}$ as described in previous two families of Steklov eigenfunctions.

Next we move on to the boundary conditions of y . If we apply (3.18) to $s_k(x, y) = \cos(\nu x + \frac{k\pi}{2}) \cosh(\nu y)$, then we arrive at

$$-\nu \cos(\nu x + \frac{k\pi}{2}) \sinh(-\nu Lh + \theta_2) = \delta \cos(\nu x + \frac{k\pi}{2}) \cosh(-\nu Lh + \theta_2) \quad (3.34)$$

Then we obtain

$$\delta = -\nu \tanh(-\nu Lh + \theta_2) \quad (3.35)$$

The boundary condition at $y = Lh$, (3.21) yields

$$\nu \cos(\nu x + \frac{k\pi}{2}) \sinh(\nu Lh + \theta_2) = \delta \cos(\nu x + \frac{k\pi}{2}) \cosh(\nu Lh + \theta_2) \quad (3.36)$$

This becomes

$$\delta = \nu \tanh(\nu Lh + \theta_2) \quad (3.37)$$

Then θ_2 may be found from combining (3.35) and (3.37)

$$\nu \tanh(-\nu Lh + \theta_2) + \nu \tanh(\nu Lh + \theta_2) = \nu \sinh(2\theta_2) = 0 \quad (3.38)$$

It follows $\theta_2 = 0$. Here we shall list eigenfunctions $s^{(III)}(x, y)$, eigenvalues $\delta_k^{(III)}$, and $\nu_k^{(III)}$ with $D_k^{(III)}(\nu)$ corresponding to $k \pmod{2}$ for the family (III).

When $k \equiv 0 \pmod{2}$, $s_{2k}^{(III)}(x, y) = \cos(\nu_k^{(III)} x) \cosh(\nu_k^{(III)} y)$

$$\delta_{2k}^{(III)} = -\nu_k^{(III)} \tan(\nu_k^{(III)} L)$$

$\nu_k^{(III)}$ is the k -th solution of $D_0^{(III)}(\nu) = 0$

with $D_0^{(III)}(\nu) := \tanh(\nu Lh) + \tan(\nu L)$

When $k \equiv 1 \pmod{2}$, $s_{2k+1}^{(III)}(x, y) = -\sin(\nu_k^{(III)} x) \cosh(\nu_k^{(III)} y)$

$\delta_{2k+1}^{(III)} = \nu_k^{(III)} \cot(\nu_k^{(III)} L)$

$\nu_k^{(III)}$ is the k-th solution of $D_1^{(III)}(\nu) = 0$

with $D_1^{(III)}(\nu) := \tanh(\nu Lh) - \cot(\nu L)$

The followings are the family (IV).

When $k \equiv 0 \pmod{2}$, $s_{2k}^{(IV)}(x, y) = \cosh(\nu_k^{(IV)} x) \cos(\nu_k^{(IV)} y)$

$\delta_{2k}^{(IV)} = -\nu_k^{(IV)} \tan(\nu_k^{(IV)} Lh)$

$\nu_k^{(IV)}$ is the k-th solution of $D_0^{(IV)}(\nu) = 0$

with $D_0^{(IV)}(\nu) := \tanh(\nu L) + \tan(\nu Lh)$

When $k \equiv 1 \pmod{2}$, $s_{2k+1}^{(IV)}(x, y) = -\cosh(\nu_k^{(IV)} x) \sin(\nu_k^{(IV)} y)$

$\delta_{2k+1}^{(IV)} = \nu_k^{(IV)} \cot(\nu_k^{(IV)} Lh)$

$\nu_k^{(IV)}$ is the k-th solution of $D_1^{(IV)}(\nu) = 0$

with $D_1^{(IV)}(\nu) := \tanh(\nu L) - \cot(\nu Lh)$

3.3 The Description of Steklov Eigenfunctions and Determining Equations

In this work, the Steklov eigenfunctions of the forms $\sin(\nu x) \sinh(\nu y)$ and $\cos(\nu x) \sinh(\nu y)$ are denoted by the ssh and csh Steklov eigenfunctions, respectively. Similarly Steklov

3.3 THE DETERMINING EQUATIONS

eigenfunctions which have the forms $\sin(\nu x) \cosh(\nu y)$ and $\cos(\nu x) \cosh(\nu y)$ will be named by the sch and cch Steklov eigenfunctions, respectively. We use this naming tradition for the rest of other eigenfunctions. The chs, chc, shs, and shc Steklov eigenfunctions represent respective eigenfunctions which of the forms $\cosh(\nu x) \sin(\nu y)$, $\cosh(\nu x) \cos(\nu y)$, $\sinh(\nu x) \sin(\nu y)$, and $\sinh(\nu x) \cos(\nu y)$.

The Steklov eigenfunctions described in the previous chapter have continuous traces on the boundary. Table (3.1) shows that which Steklov eigenfunctions are even and odd about the center on each side.

Steklov eigenfunction	on Γ_2 and Γ_4	on Γ_1 and Γ_3
ssh and shs	odd in x	odd in y
cch and chc	even in x	even in y
sch and shc	odd in x	even in y
chs and csh	even in x	odd in y

Table 3.1: The symmetry of each Steklov eigenfunction on the boundary

Now, we shall describe the determining equations. Consider $z = \coth(w)$ and $z = \tanh(w)$. For positive w, these two functions have a horizontal asymptote $z=1$. Then after a few solutions of the equations $D_0^{(I)}(\nu) = 0$ and $D_1^{(III)}(\nu) = 0$, they have same solutions. This also holds for $D_1^{(I)}(\nu) = 0$ and $D_0^{(III)}(\nu) = 0$, $D_0^{(II)}(\nu) = 0$ and $D_1^{(IV)}(\nu) = 0$, $D_1^{(II)}(\nu) = 0$ and $D_0^{(IV)}(\nu) = 0$. In addition, for the case when $h=1$, $D_0^{(I)}(\nu) = D_0^{(II)}(\nu)$, $D_1^{(I)}(\nu) = D_1^{(II)}(\nu)$, $D_0^{(III)}(\nu) = D_0^{(IV)}(\nu)$, and $D_1^{(III)}(\nu) = D_1^{(IV)}(\nu)$. Here we provide Figures (3.2)-(3.5) which show solutions of each determining equation for the case when $L = h = 1$.

We implement the fixed-point iteration method(see Section 6.1.4 of [7]) on Matlab with a tolerance, $2.2204e^{-16}$. We observe that ν_2 on Figure (3.2) and ν_3 on Figure (3.5) are same when they are evaluated to 4 decimal places. Also ν_2 and ν_3 on Figures

3.3 THE DETERMINING EQUATIONS

(3.3) and (3.4) are same, respectively.

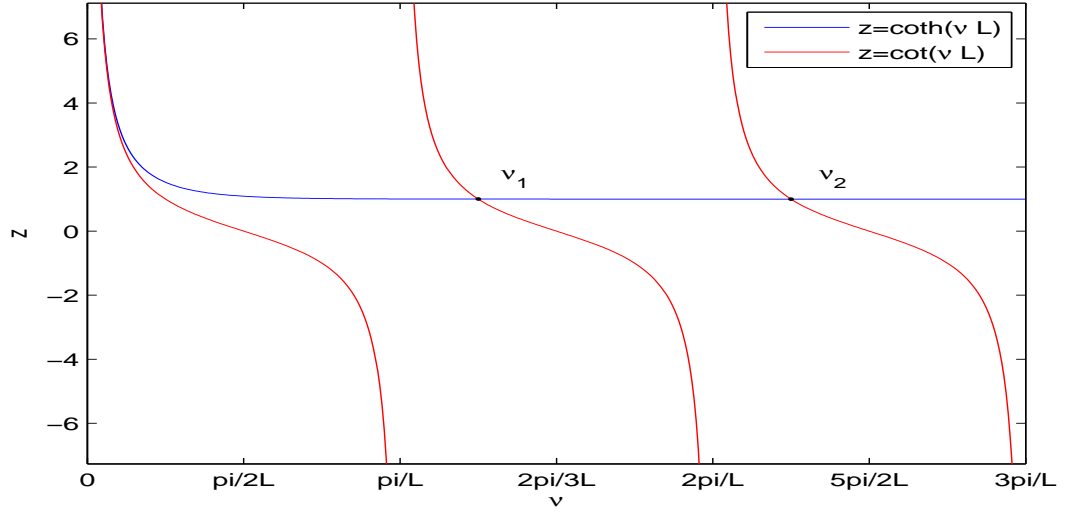


Figure 3.2: Solutions of $D_0^{(I)}(\nu) = 0$ or $D_0^{(II)}(\nu) = 0$. $\nu_1 = 3.9266$ and $\nu_2 = 7.0686$.

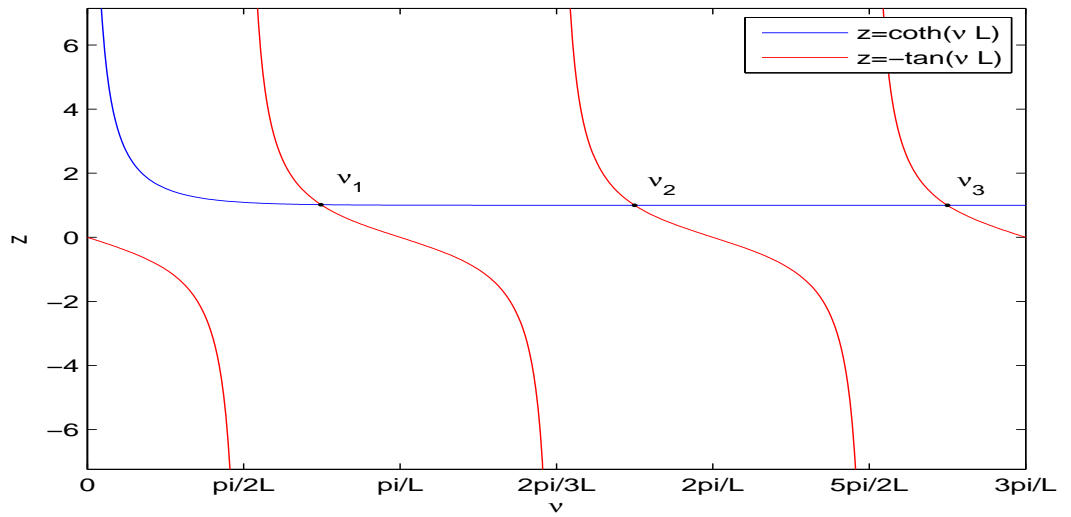


Figure 3.3: Solutions of $D_1^{(I)}(\nu) = 0$ or $D_1^{(II)}(\nu) = 0$. $\nu_1 = 2.347$, $\nu_2 = 5.4978$, and $\nu_3 = 8.6394$.

3.3 THE DETERMINING EQUATIONS

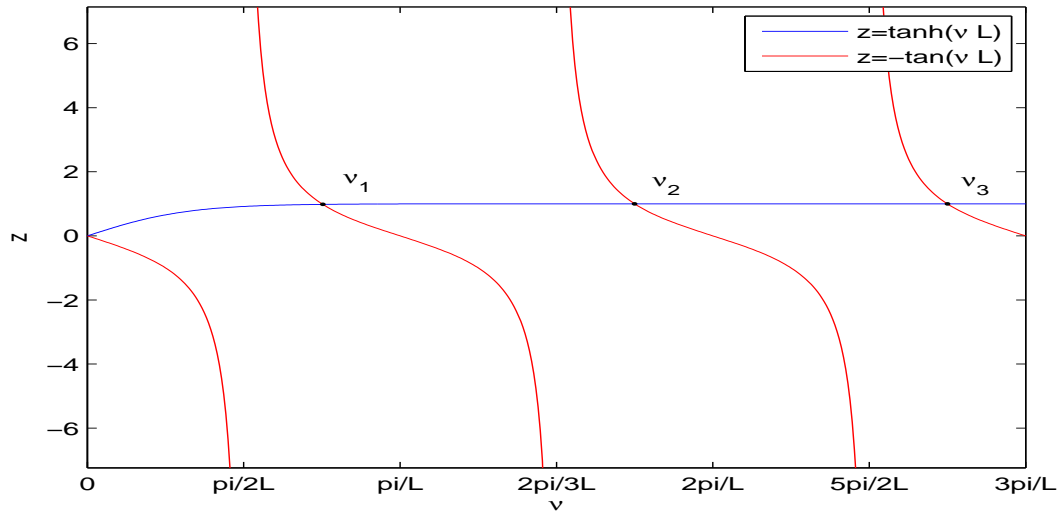


Figure 3.4: Solutions of $D_0^{(III)}(\nu) = 0$ or $D_0^{(IV)}(\nu) = 0$. $\nu_1 = 2.365$, $\nu_2 = 5.4978$, and $\nu_3 = 8.6394$.

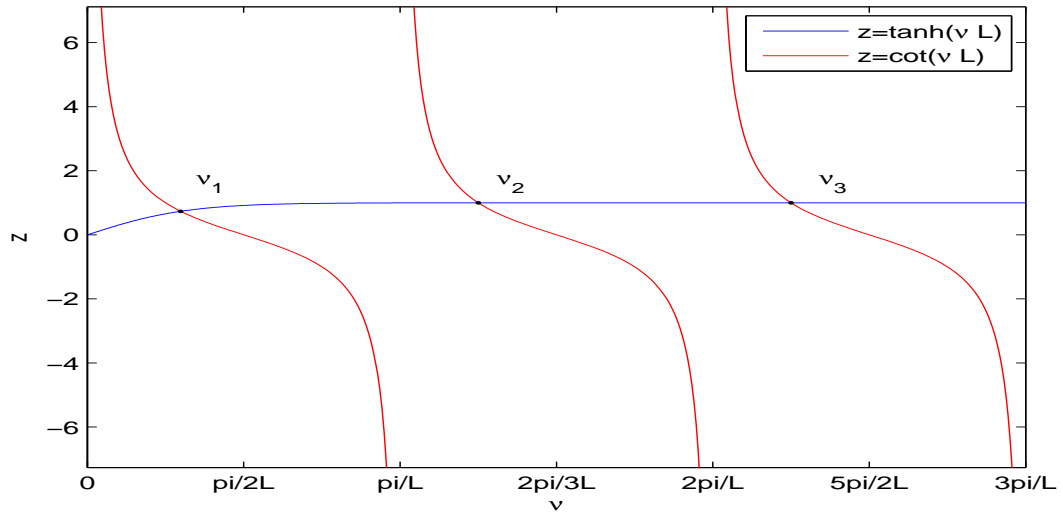


Figure 3.5: Solutions of $D_1^{(III)}(\nu) = 0$ or $D_1^{(IV)}(\nu) = 0$. $\nu_1 = 0.93755$, $\nu_2 = 3.9274$, and $\nu_3 = 7.0686$.

3.4 A Special Steklov Eigenvalue and a Corresponding Steklov Eigenfunction

In this section, we look for a special Steklov eigenvalue and a corresponding eigenfunction quite different from four families described in the preceding section. These may be found if we start with letting $b = \nu = 0$ on (3.6). Then we have two ordinary equations, $V'' = 0$ and $W'' = 0$ on Ω . It means that $s(x, y) = (Ax + B)(Cy + D)$ for constants A, B, C , and D . In order to find those constants, we apply the boundary condition. (3.8) yields

$$-A(Cy + D) = \delta(-AL + B)(Cy + D) \quad (3.39)$$

Or,

$$A(1 - \delta L) + \delta B = 0 \quad (3.40)$$

Since all strictly positive eigenvalues are concerned, $\delta L = 1$ and $B = 0$. Same results may obtained from (3.11). For C and D , from (3.18) or (3.21) we have

$$-(Ax)C = \delta(Ax)(-CLh + D) \quad (3.41)$$

Then $\delta Lh = 1$ and $D = 0$. It implies that when $h=1$, additional Steklov eigenvalue, $\delta = \frac{1}{L}$ with the associated Steklov eigenfunction, $s(x, y) = xy$ will be obtained and this eigenvalue is simple. This functions is linear on each segment of the boundary.

3.5 The Ordering of Eigenfunctions and Eigenvalues

We shall index the first n Steklov eigenvalues so that $0 = \delta_0 < \delta_1 \leq \delta_2 \leq \dots \leq \delta_{n-1}$. Theorem 7.2 of [1] yields that each Steklov eigenvalue δ_i has finite multiplicity and $\delta_i \rightarrow \infty$ as $i \rightarrow \infty$. Let s_i be a Steklov eigenfunction corresponding to δ_i for $0 \leq i \leq n - 1$. The following is a list of first 13 Steklov eigenfunctions after $s_0(x, y) \equiv 1$ with corresponding ν_i and Steklov eigenvalues δ_i when $L = h = 1$. They came from Sections 3.2 and 3.3.

$$s_1(x, y) = -\sin(0.93755x) \cosh(0.93755y), \quad \nu_1 = 0.93755, \quad \delta_1 = 0.68825$$

$$s_2(x, y) = -\cosh(0.93755x) \sin(0.93755y), \quad \nu_2 = 0.93755, \quad \delta_2 = 0.68825$$

$$s_3(x, y) = xy, \quad \nu_3 = 0, \quad \delta_3 = 1.0000$$

$$s_4(x, y) = \cos(2.365x) \cosh(2.365y), \quad \nu_4 = 2.365, \quad \delta_4 = 2.3236$$

$$s_5(x, y) = \cosh(2.365x) \cos(2.365y), \quad \nu_5 = 2.365, \quad \delta_5 = 2.3236$$

$$s_6(x, y) = \cos(2.347x) \sinh(2.347y), \quad \nu_6 = 2.347, \quad \delta_6 = 2.3904$$

$$s_7(x, y) = \sinh(2.347x) \cos(2.347y), \quad \nu_7 = 2.347, \quad \delta_7 = 2.3904$$

$$s_8(x, y) = -\sin(3.9274x) \cosh(3.9274y), \quad \nu_8 = 3.9274, \quad \delta_8 = 3.9243$$

$$s_9(x, y) = -\cosh(3.9274x) \sin(3.9274y), \quad \nu_9 = 3.9274, \quad \delta_9 = 3.9243$$

$$s_{10}(x, y) = \sin(3.9266x) \sinh(3.9266y), \quad \nu_{10} = 3.9266, \quad \delta_{10} = 3.9297$$

$$s_{11}(x, y) = \sinh(3.9266x) \sin(3.9266y), \quad \nu_{11} = 3.9266, \quad \delta_{11} = 3.9297$$

$$s_{12}(x, y) = \cos(5.4978x) \cosh(5.4978y), \quad \nu_{12} = 5.4978, \quad \delta_{12} = 5.4976$$

$$s_{13}(x, y) = \cosh(5.4978x) \cos(5.4978y), \quad \nu_{13} = 5.4978, \quad \delta_{13} = 5.4976$$

3.5 THE ORDERING OF EIGENFUNCTIONS AND EIGENVALUES

We observe that in this order, δ_0 and δ_3 are simple and the other Steklov eigenvalues are double, respectively. The next eigenvalues in this case are in Table (3.2).

j	14	15	16	17	18	19	20	21
δ_j	5.4976	5.4976	7.0686	7.0686	7.0686	7.0686	8.6394	8.6394
j	22	23	24	25	26	27	28	29
δ_j	8.6394	8.6394	10.21	10.21	10.21	10.2	11.781	11.781
j	30	31	32	33	34	35	36	37
δ_j	11.781	11.781	13.352	13.352	13.352	13.352	14.922	14.922

Table 3.2: Steklov eigenvalues

Table (3.2) shows that after 13th eigenvalue, these eigenvalues appear to have multiplicity 4 when evaluated to 4 decimal places. In Table (3.3), we see that when $h=0.9$, Steklov eigenvalues δ_i have multiplicity 2 for $i \geq 16$ and when $h=0.8$ and $h=0.5$, δ_i have multiplicity 2 for $i \geq 14$, respectively.

Let 50 eigenvalues be $0 = \delta_0 < \delta_1 < \delta_2 < \dots < \delta_j < \dots < \delta_{49}$. In Figure (3.6), we see that Steklov eigenvalues are increasing linearly against j with respective slopes 39.542($h=1$), 42.177($h=0.9$), 44.471($h=0.8$), and 53.454($h=0.5$).

3.5 THE ORDERING OF EIGENFUNCTIONS AND EIGENVALUES

	h=0.9	h=0.8	h=0.5
δ_0	0	0	0
δ_1	0.67143	0.65105	0.55531
δ_2	0.78189	0.8991	1.5271
δ_3	1.0579	1.1361	1.6294
δ_4	2.3046	2.2749	2.0522
δ_5	2.4417	2.4467	2.7811
δ_6	2.5964	2.9325	3.7967
δ_7	2.6403	2.9582	4.0672
δ_8	3.9118	3.9142	4.7117
δ_9	3.9328	3.9397	4.7131
δ_{10}	4.3621	4.9083	5.4572
δ_{11}	4.3645	4.9092	5.5391
δ_{12}	5.4974	5.4963	7.0575
δ_{13}	5.4984	5.4993	7.0799
δ_{14}	6.1087	6.8724	7.8542
δ_{15}	6.1088	6.8724	7.8542
δ_{16}	7.0688	7.0687	8.6468
δ_{17}	7.0688	7.0687	8.6468
δ_{18}	7.8544	8.6399	10.211
δ_{19}	7.8544	8.6399	10.211
δ_{20}	8.6401	8.8363	10.997
δ_{21}	8.6401	8.8363	10.997
δ_{22}	9.6004	10.211	11.782
δ_{23}	9.6004	10.211	11.782
δ_{24}	10.212	10.801	13.354
δ_{25}	10.212	10.801	13.354

Table 3.3: First 26 Steklov eigenvalues for h=0.9, 0.8, and 0.5 when L=1

3.5 THE ORDERING OF EIGENFUNCTIONS AND EIGENVALUES

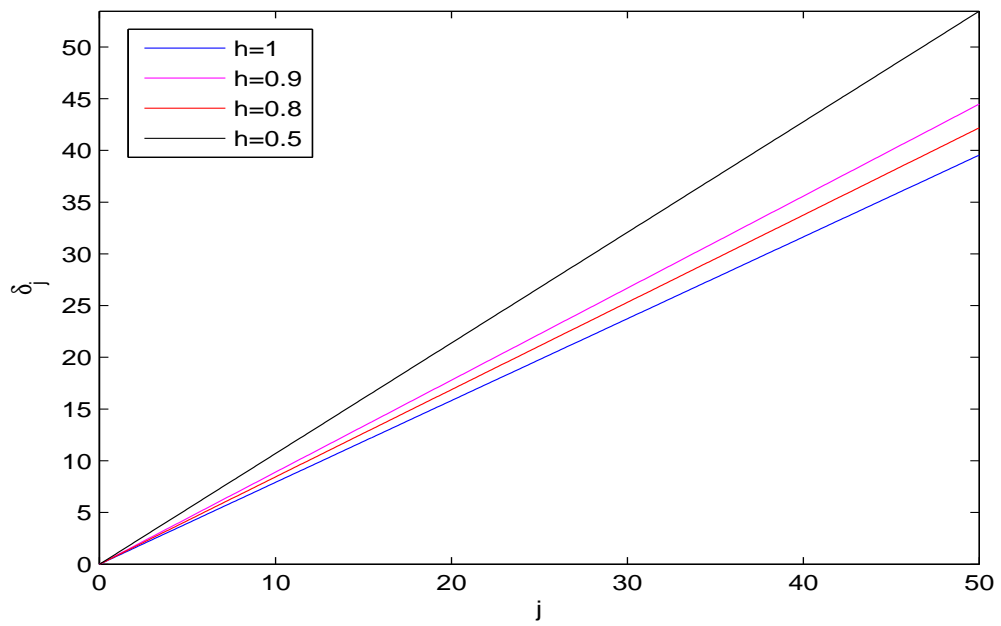


Figure 3.6: Distinct eigenvalues against j

3.6 Normalized Steklov Eigenfunctions

The Steklov eigenfunctions $s_i \in H^1(\Omega)$ described in the previous section have continuous traces on the boundary $\partial\Omega$. We define the boundary normalized Steklov eigenfunctions to have $\int_{\partial\Omega} \hat{s}_i(x, y)^2 d\sigma = 1$, i.e.,

$$\hat{s}_i(x, y) := \|s_i\|_{2,\partial\Omega}^{-1} s_i(x, y) \text{ for } (x, y) \in \overline{\Omega}, \text{ and } i \geq 0 \tag{3.42}$$

They also satisfy $\int_{\partial\Omega} \hat{s}_i \hat{s}_j d\sigma = 0$ when $i \neq j$. We notice that $\hat{s}_0 \equiv 1$ so that for $i > 0$, $\int_{\partial\Omega} \hat{s}_i d\sigma = \langle \hat{s}_i, 1 \rangle_{2,\partial\Omega} = \langle \hat{s}_i, \hat{s}_0 \rangle_{2,\partial\Omega} = 0$, i.e., the mean value of \hat{s}_i on the boundary is zero. Theorem 4.1 of [2] says that $\hat{\mathcal{S}} := \{\hat{s}_i : i \geq 0\}$ is a maximal orthonormal set in $L^2(\partial\Omega, d\sigma)$ and a maximal orthogonal set in $H^1(\Omega)$. Again, we let $L = h = 1$. Consider \hat{s}_i , $1 \leq i \leq 13$. The following table gives their amplitudes ,maximum and minimum values on the boundary, and values at each of corners.

	amplitude	max	min	$\hat{s}(-1, -1)$	$\hat{s}(1, -1)$	$\hat{s}(1, 1)$	$\hat{s}(-1, 1)$
\hat{s}_1	2.8284	1.4142	-1.4142	1.4142	-1.4142	-1.4142	1.4142
\hat{s}_2	2.82842	1.4142	-1.4142	1.4142	1.4142	-1.4142	-1.4142
\hat{s}_3	3.4642	1.7321	-1.7321	1.7321	-1.7321	1.7321	-1.7321
\hat{s}_4, \hat{s}_5	3.3967	1.9825	-1.4142	-1.4142	-1.4142	-1.4142	-1.4142
\hat{s}_6	4.0371	2.0185	-1.4142	1.4142	1.4142	-1.4142	-1.4142
\hat{s}_7	4.0371	2.0185	1.4142	1.4142	-1.4142	-1.4142	1.4142
\hat{s}_8	3.9984	1.9992	-1.9992	-1.4142	1.4142	1.4142	-1.4142
\hat{s}_9	3.9984	1.9992	-1.9992	-1.4142	-1.4142	1.4142	1.4142
$\hat{s}_{10}, \hat{s}_{11}$	4.0015	2.0007	-2.0007	-1.4142	1.4142	-1.4142	1.4142
$\hat{s}_{12}, \hat{s}_{13}$	4	2	-2	1.4142	1.4142	1.4142	1.4142

Table 3.4: Normalized Steklov eigenfunctions

Table (3.4) shows that at each corner, for $1 \leq i \leq 13$, \hat{s}_i has a same absolute value, 1.4142 except for \hat{s}_3 . Figures (3.7)-(3.10) graph the normalized Steklov eigenfunctions

3.6 NORMALIZED STEKLOV EIGENFUNCTIONS

on each side. We compare \hat{s}_i for $i \in [1, 3, 4, 6, 8, 10, 12]$ to see how they oscillate on each side. Same result will be observed for $i \in [2, 5, 7, 9, 11, 13]$. On each graph, except for \hat{s}_4 some eigenfunctions are multiplied by -1 so that all eigenfunctions have same value at $x = -1$ or $y = -1$. Figures (3.11)-(3.13) represent respective contour plots of successive Steklov eigenfunctions \hat{s}_i , $1 \leq i \leq 13$ and show that the eigenfunctions are very “flat” in the interior of the rectangle.

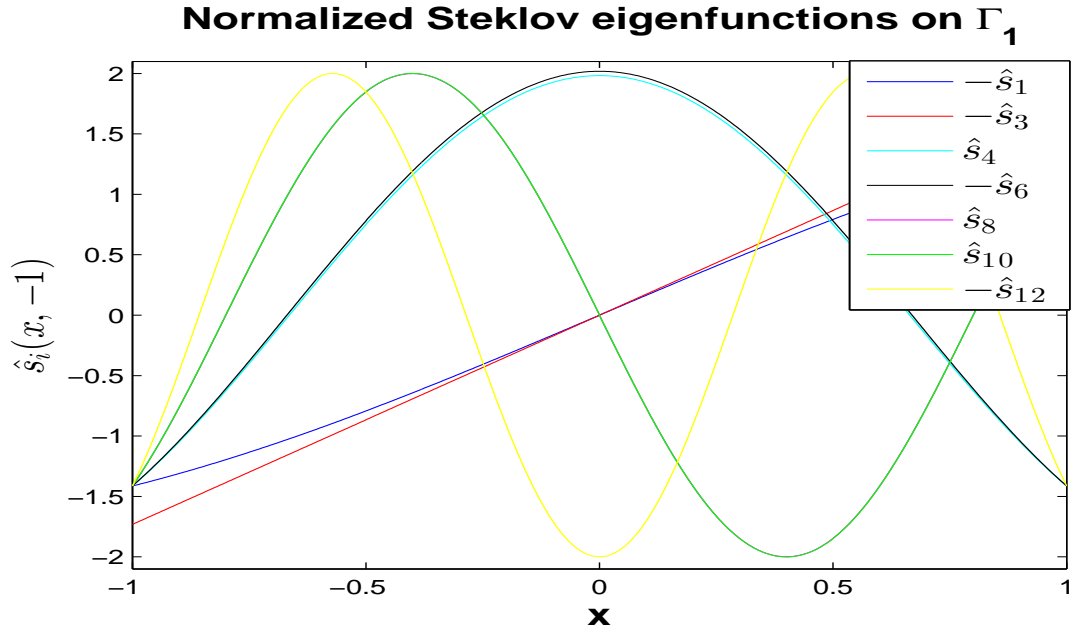


Figure 3.7: Normalized Steklov eigenfunctions \hat{s}_i on Γ_1 for $i \in [1, 3, 4, 6, 8, 10, 12]$

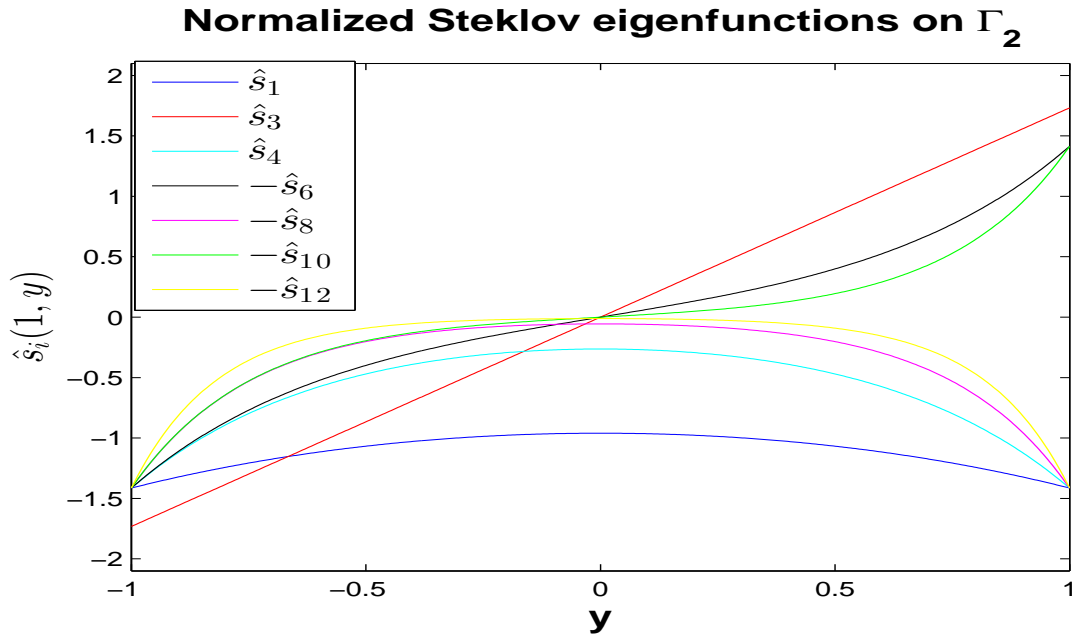


Figure 3.8: Normalized Steklov eigenfunctions \hat{s}_i on Γ_2 for $i \in [1, 3, 4, 6, 8, 10, 12]$

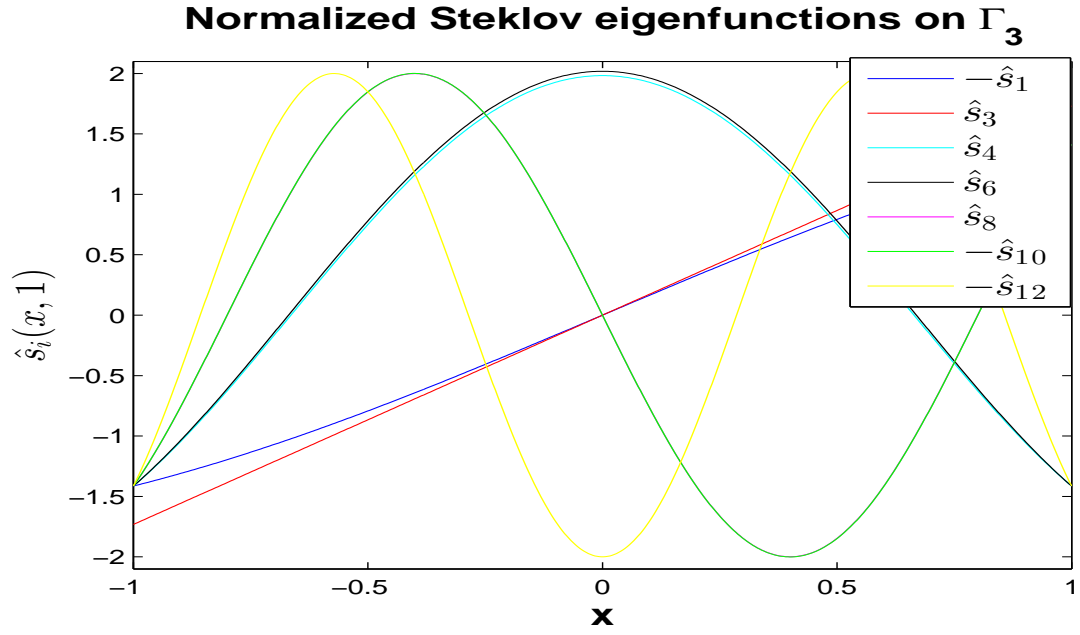


Figure 3.9: Normalized Steklov eigenfunctions \hat{s}_i on Γ_3 for $i \in [1, 3, 4, 6, 8, 10, 12]$

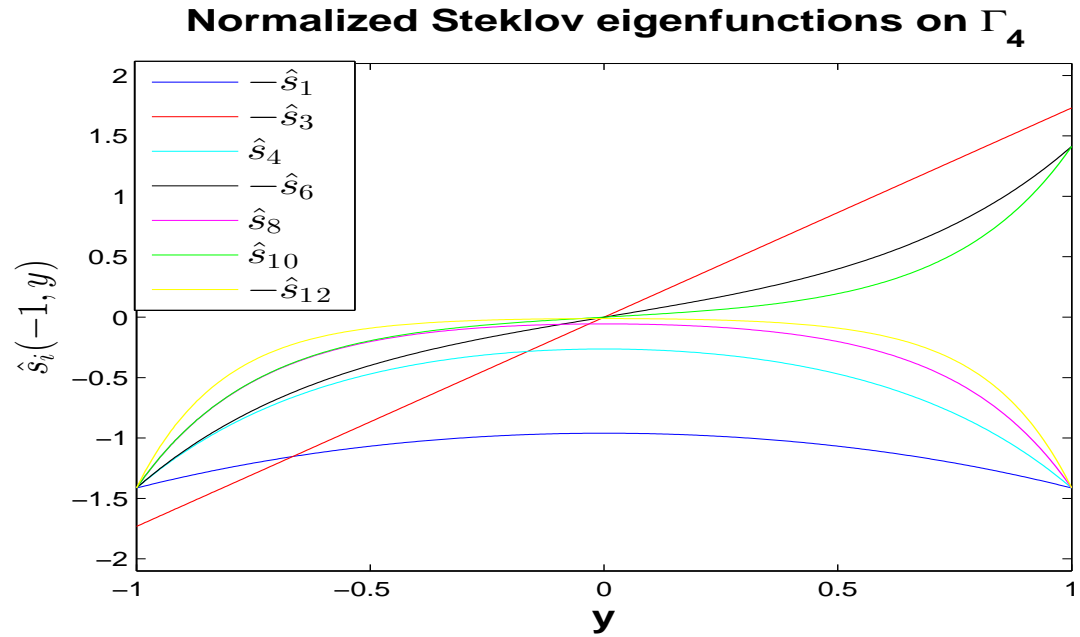


Figure 3.10: Normalized Steklov eigenfunctions \hat{s}_i on Γ_4 for $i \in [1, 3, 4, 6, 8, 10, 12]$

3.6 NORMALIZED STEKLOV EIGENFUNCTIONS

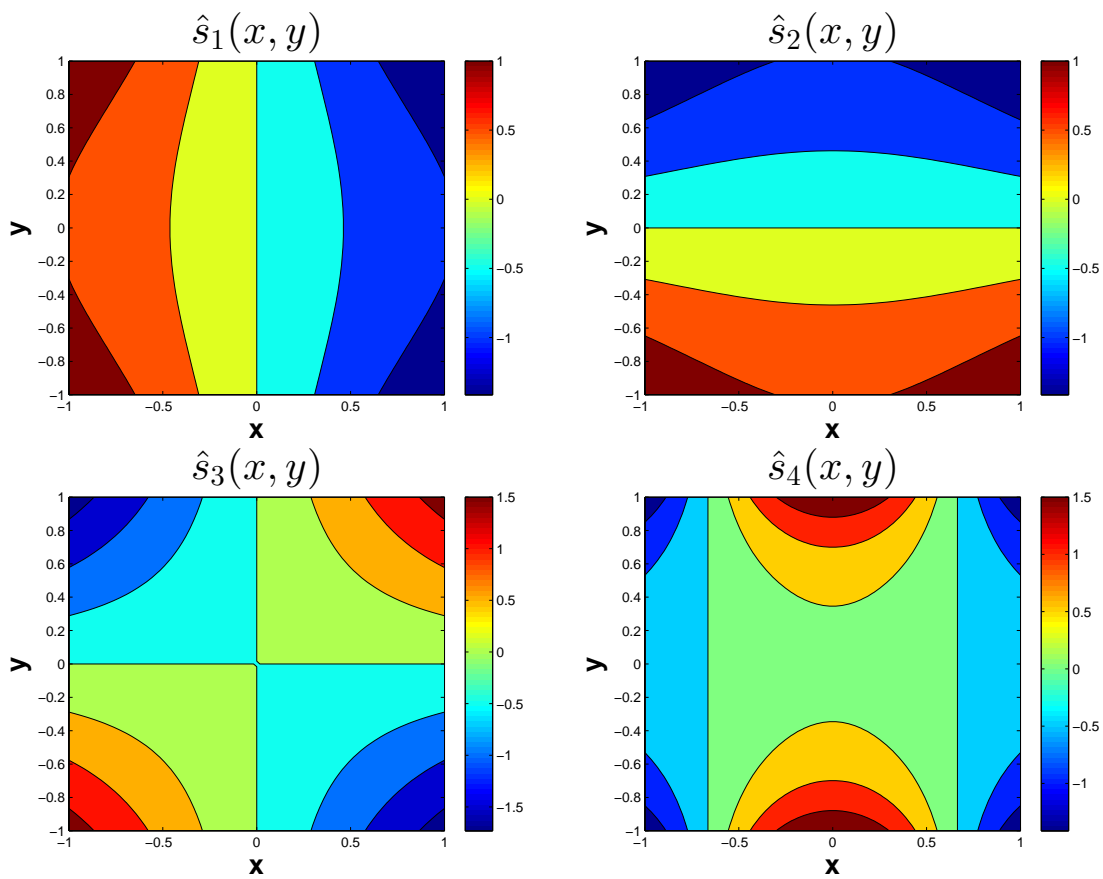


Figure 3.11: Contour plots of Steklov eigenfunctions \hat{s}_1 (Left top), \hat{s}_2 (Right top), \hat{s}_3 (Left bottom), and \hat{s}_4 (Right bottom).

3.6 NORMALIZED STEKLOV EIGENFUNCTIONS

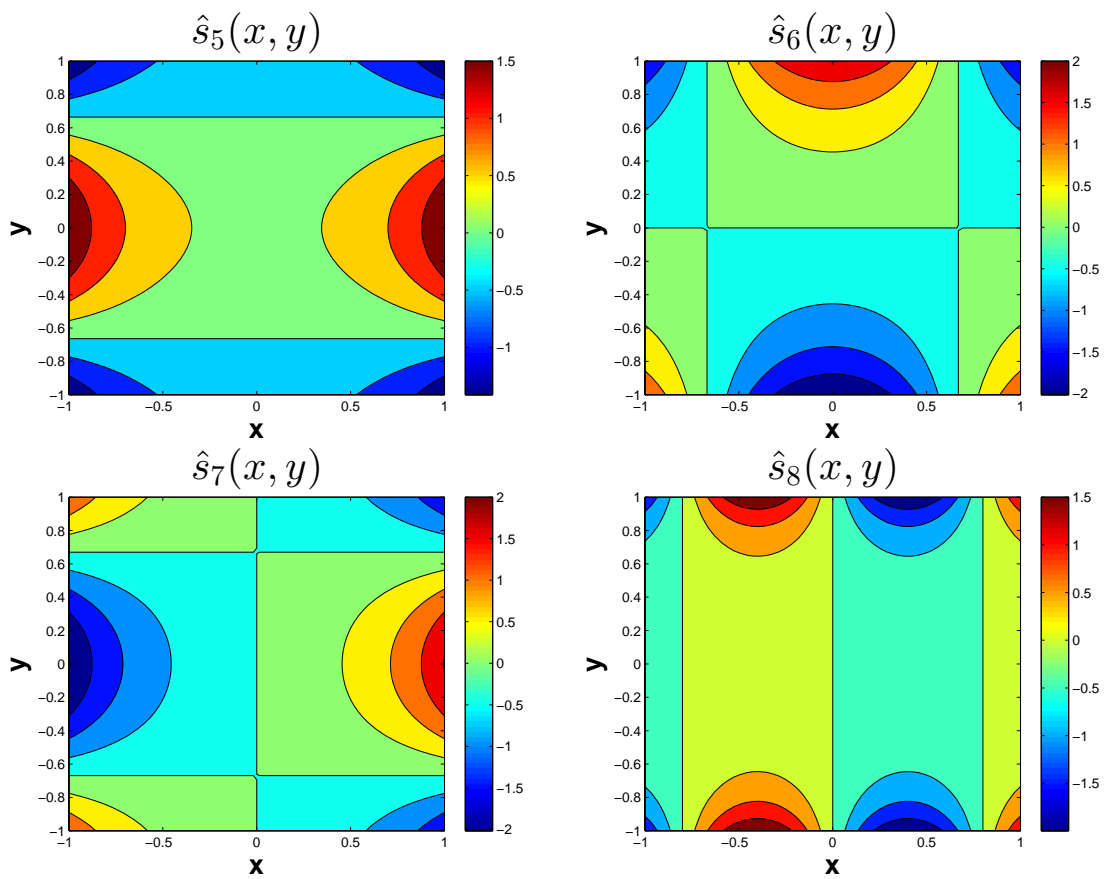


Figure 3.12: Contour plots of Steklov eigenfunctions \hat{s}_5 (Left top), \hat{s}_6 (Right top), \hat{s}_7 (Left bottom), and \hat{s}_8 (Right bottom).

3.6 NORMALIZED STEKLOV EIGENFUNCTIONS

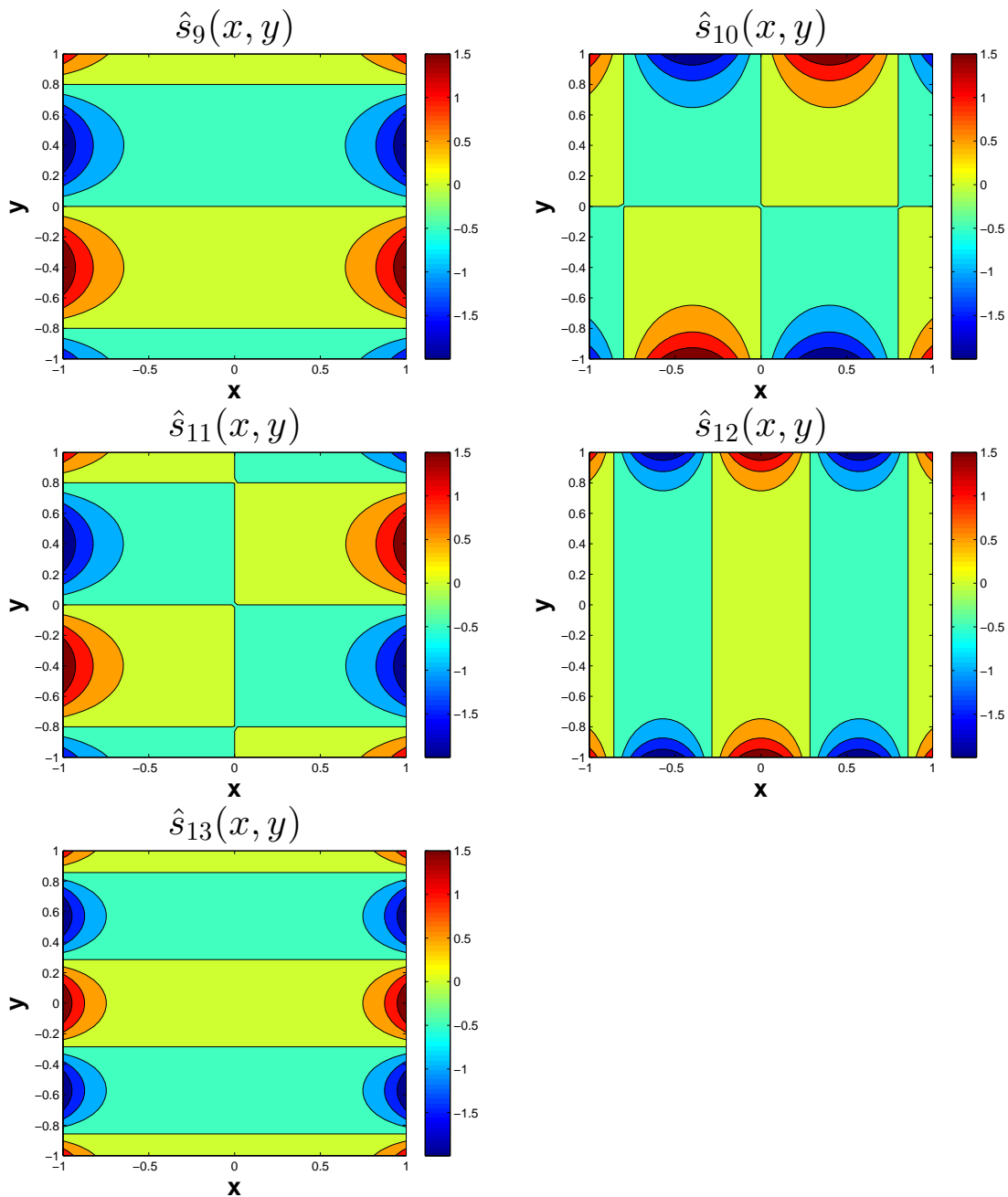


Figure 3.13: Contour plots of Steklov eigenfunctions \hat{s}_9 (Left top), \hat{s}_{10} (Right top), \hat{s}_{11} (Left middle), \hat{s}_{12} (Right middle), and \hat{s}_{13} (Left bottom).

Chapter 4

Spectral Representations for Harmonic Functions

4.1 The Steklov and Neumann Expansions of Harmonic Functions

The Neumann eigenproblem is that of finding non-trivial solutions of the problem

$$-\Delta n = \rho n \quad \text{in } \Omega \tag{4.1}$$

$$D_\nu n = 0 \quad \text{on } \partial\Omega \tag{4.2}$$

where $\Omega = [-L, L] \times [-Lh, Lh]$. The weak form of (4.1)-(4.2) is to find the real values ρ such that there is a non-zero solution n in $H^1(\Omega)$ of

$$\int_{\Omega} \nabla n \cdot \nabla v \, dx = \rho \int_{\Omega} n v \, dx \quad \text{for all } v \in H^1(\Omega) \tag{4.3}$$

4.1 THE STEKLOV EXPANSION

The function $n(x, y)$ will be called the *Neumann eigenfunction* corresponding to the Neumann eigenvalue ρ .

The explicit formulae of solutions of this problem are well known (see Chapter 4 of [20]). The Neumann eigenvalues are $\rho_{jk} = (\frac{j\pi}{2L})^2 + (\frac{k\pi}{2Lh})^2$ for $j, k \geq 0$ and corresponding Neumann eigenfunctions are $n_{jk}(x, y) = \cos(\frac{j\pi}{2L}(x + L)) \cos(\frac{k\pi}{2Lh}(y + Lh))$ for $j, k \geq 0$. Let the first i Neumann eigenvalues be $0 = \rho_0 \leq \rho_1 \leq \rho_2 \leq \dots \leq \rho_{i-1}$ and n_0, n_1, \dots, n_{i-1} be a corresponding set of orthonormal eigenfunctions in $L^2(\Omega)$ with respect to the inner product defined in Chapter 2. Then the set $\mathcal{N} := \{n_i : i \geq 0\}$ is a maximal orthonormal set in $L^2(\Omega)$ and an orthogonal subset of $H^1(\Omega)$ (see Section 11.3 of [20]).

Let $\tilde{f}_M := \sum_{i=0}^M \tilde{c}_i n_i(x, y)$, $M \geq 1$ with $\tilde{c}_i := \langle f, n_i(x, y) \rangle_{2,\Omega}$ be the M -th partial sum of the Neumann expansion of f . Then we see that

$$\|\tilde{f}_M\|_{1,2}^2 = \sum_{i=0}^M \left[\int_{\Omega} \tilde{c}_i^2 |\nabla n_i|^2 dx + \int_{\Omega} \tilde{c}_i^2 n_i^2 dx \right] \quad (4.4)$$

$$= \sum_{i=0}^M (\tilde{c}_i^2 \rho_i + \tilde{c}_i^2) \quad (4.5)$$

$$= \sum_{i=0}^M \tilde{c}_i^2 (\rho_i + 1) \quad (4.6)$$

The second equality holds from (4.3). This implies that a function f is in $H^1(\Omega)$ if and only if

$$\lim_{M \rightarrow \infty} \sum_{i=0}^M \tilde{c}_i^2 (\rho_i + 1) < \infty \quad (4.7)$$

When $f \in H^1(\Omega)$ then the sequence $\{\tilde{f}_M\}$ converges to f in $H^1(\Omega)$. These results may be summarized as follows.

Theorem 4.1. *Assume Ω , $\partial\Omega$, ρ_i , n_i , and \tilde{c}_i are defined as above. Then a function f*

4.1 THE STEKLOV EXPANSION

is in $H^1(\Omega)$ if and only if f satisfies (4.7). In this case, the sequence $\{f_M\}$ converges strongly in the H^1 -norm.

An expression of form

$$f(x, y) := \lim_{M \rightarrow \infty} \sum_{i=0}^M c_i \hat{s}_i(x, y) \quad \text{with } c_i := \langle f, \hat{s}_i \rangle_{2, \partial\Omega} \quad (4.8)$$

will be called the *Steklov expansion* of f . Let $f_M(x, y) := \sum_{i=0}^M c_i \hat{s}_i(x, y)$, $M \geq 1$ be the M -th partial sum of the Steklov expansion of f . Then

$$\|f_M\|_{\partial}^2 = \sum_{i=0}^M \left[\int_{\Omega} c_i^2 |\nabla \hat{s}_i|^2 dx + \int_{\partial\Omega} c_i^2 \hat{s}_i^2 d\sigma \right] \quad (4.9)$$

$$= \sum_{i=0}^M (c_i^2 |\partial\Omega| \delta_i + c_i^2) \quad (4.10)$$

$$= \sum_{i=0}^M c_i^2 (|\partial\Omega| \delta_i + 1) \quad (4.11)$$

The second equality holds from (3.3). This shows that (4.8) represents an H^1 -harmonic function if and only if

$$\lim_{M \rightarrow \infty} \sum_{i=0}^M c_i^2 (|\partial\Omega| \delta_i + 1) < \infty \quad (4.12)$$

When $f \in H^1(\Omega)$ then the sequence $\{f_M\}$ converges to f in $H^1(\Omega)$. Above results may be summarized as follows.

Theorem 4.2. *Assume Ω , $\partial\Omega$, δ_i , and \hat{s}_i are defined in Chapter 3 and c_i is defined as above. Then a harmonic function f is in $H^1(\Omega)$ if and only if f satisfies (4.12). In this case, the sequence $\{f_M\}$ converges strongly in the ∂ -norm on $H^1(\Omega)$.*

This is a special case of Corollary 9.5 of [1].

4.2 Relative Errors for the Steklov Expansion

As described in the preceding section, a $H^1(\Omega)$ function f has representations in series involving either the Steklov and Neumann eigenfunctions. Here we will compare these expansions where f is a harmonic function. We consider the M -th Steklov approximation of f , namely, f_M and the M -th Neumann approximation of f , namely, \tilde{f}_M as defined in the previous section. Then Theorem 4.2 implies that $\lim_{M \rightarrow \infty} \|f - f_M\| = 0$ where the norm is either $\|\cdot\|_2$ or $\|\nabla \cdot\|_2$. However, when it comes to the Neumann expansion of a harmonic function on Ω , we suspect the convergence is very slow.

Now we perform numerical experiments to compare the Steklov expansion of f against the Neumann expansion of f . Let $L=1$, then $\Omega = [-1, 1] \times [-h, h]$. Corresponding to $h=1, 0.8$, and 0.5 , results of relative errors of two expansions of harmonic functions with respect to $\|\cdot\|_2, \|\cdot\|_\infty$, and $\|\nabla \cdot\|_2$ against M are plotted and numerical results will be presented in tables, respectively. We suspect that the graph of each relative error with respect to three norms is the decay like $CM^{-\alpha}$ for constants C and $\alpha > 0$. This α will be called the *decay power*.

4.2 RELATIVE ERRORS FOR THE STEKLOV EXPANSION

1. $f_1(x, y) := x^2 - y^2$

(i) Case: $h=1$

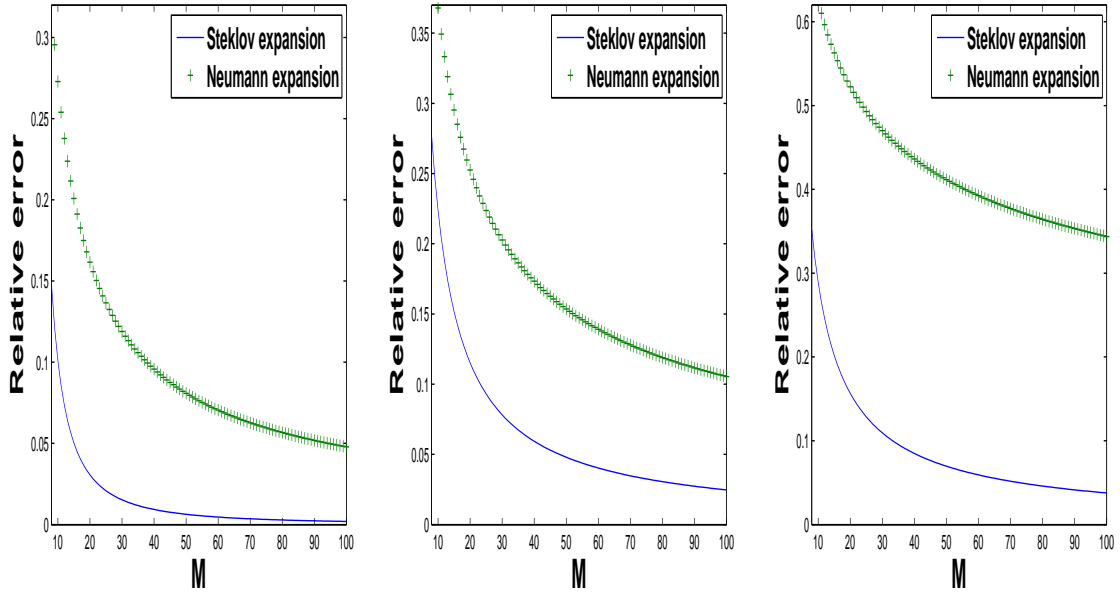


Figure 4.1: Relative errors of the M -th Steklov and Neumann approximations of f in $\|\cdot\|_2$ (left), $\|\cdot\|_\infty$ (middle), and $\|\nabla \cdot\|_2$ (right) against M .

M	Relative error in $\ \cdot\ _2$		Relative error in $\ \cdot\ _\infty$		Relative error in $\ \nabla \cdot\ _2$	
	Steklov	Neumann	Steklov	Neumann	Steklov	Neumann
8	0.13246	0.27579	0.23642	0.35997	0.32974	0.62616
16	0.046567	0.21723	0.13259	0.31893	0.1911	0.56221
48	0.0064485	0.083119	0.047911	0.15577	0.070161	0.41538
100	0.0016837	0.057443	0.024455	0.12126	0.03588	0.3668
α	1.7204	0.75587	0.95734	0.54293	0.88426	0.26002

Table 4.1: Relative errors of two approximations in three different norms corresponding to $M=8, 16, 48,$ and 100 and decay power α of each approximation

4.2 RELATIVE ERRORS FOR THE STEKLOV EXPANSION

(ii) Case: $h=0.8$

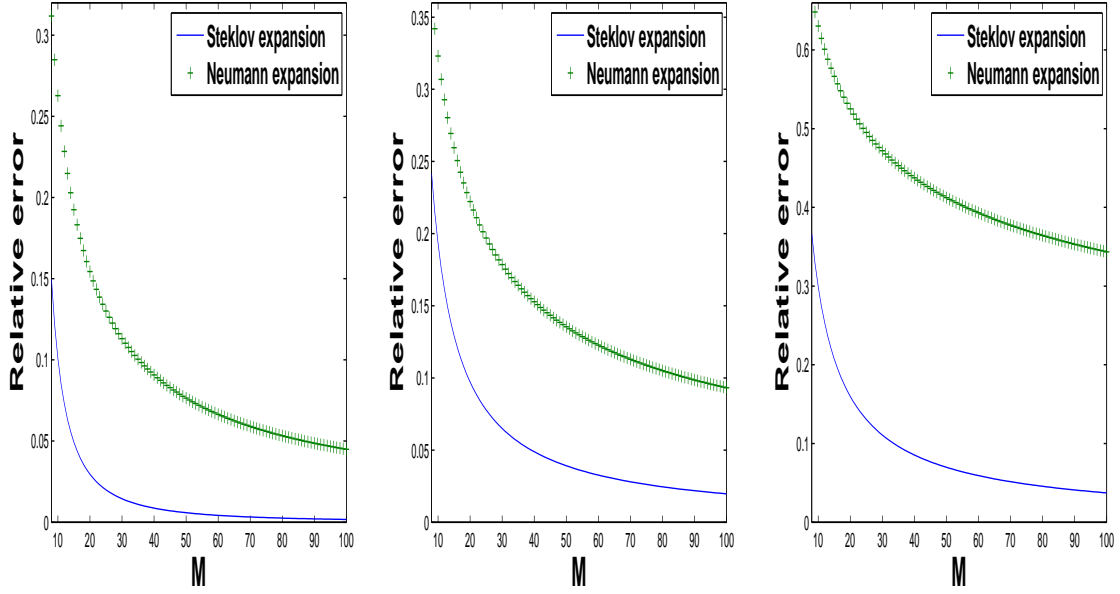


Figure 4.2: Relative errors of the M -th Steklov and Neumann approximations of f in $\|\cdot\|_2$ (left), $\|\cdot\|_\infty$ (middle), and $\|\nabla \cdot\|_2$ (right) against M .

	Relative error in $\ \cdot\ _2$		Relative error in $\ \cdot\ _\infty$		Relative error in $\ \nabla \cdot\ _2$	
	Steklov	Neumann	Steklov	Neumann	Steklov	Neumann
$M=8$	0.12637	0.26119	0.19731	0.32448	0.33178	0.62616
$M=16$	0.044385	0.17742	0.11016	0.22484	0.19229	0.54718
$M=48$	0.0069735	0.062451	0.04218	0.11577	0.076082	0.38649
$M=100$	0.0014391	0.054402	0.019058	0.1099	0.034504	0.36681
α	1.7677	0.76712	0.99223	0.54002	0.90438	0.26367

Table 4.2: Relative errors of two approximations in three different norms corresponding to $M=8, 16, 48,$ and 100 and decay power α of each expansion

4.2 RELATIVE ERRORS FOR THE STEKLOV EXPANSION

(iii) Case: $h=0.5$

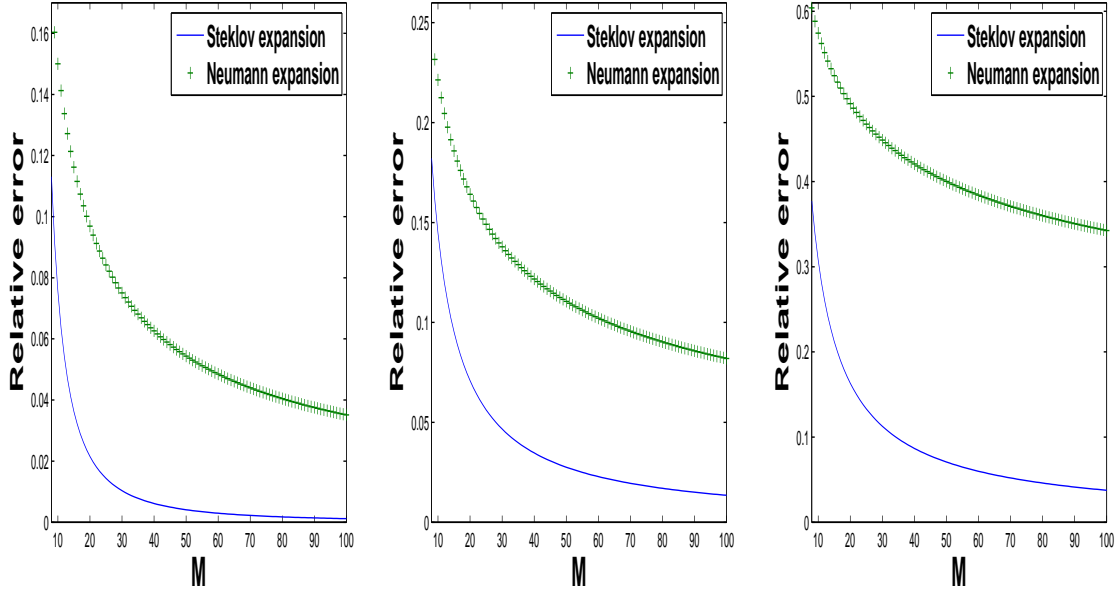


Figure 4.3: Relative errors of the M -th Steklov and Neumann approximations of f in $\|\cdot\|_2$ (left), $\|\cdot\|_\infty$ (middle), and $\|\nabla \cdot\|_2$ (right) against M .

	Relative error in $\ \cdot\ _2$		Relative error in $\ \cdot\ _\infty$		Relative error in $\ \nabla \cdot\ _2$	
	Steklov	Neumann	Steklov	Neumann	Steklov	Neumann
$M=8$	0.11485	0.17014	0.16753	0.24472	0.37291	0.6167
$M=16$	0.045657	0.11431	0.095438	0.18471	0.23943	0.52008
$M=48$	0.0040452	0.050171	0.026844	0.10409	0.070197	0.39453
$M=100$	0.0010539	0.044561	0.01368	0.097589	0.035432	0.36681
α	1.8098	0.63042	1.0303	0.43145	0.91334	0.22467

Table 4.3: Relative errors of two approximations in three different norms corresponding to $M=8, 16, 48,$ and 100 and decay power α of each expansion

4.2 RELATIVE ERRORS FOR THE STEKLOV EXPANSION

2. $f_2(x, y) := x^3 - 3xy^2$

(i) Case: $h=1$

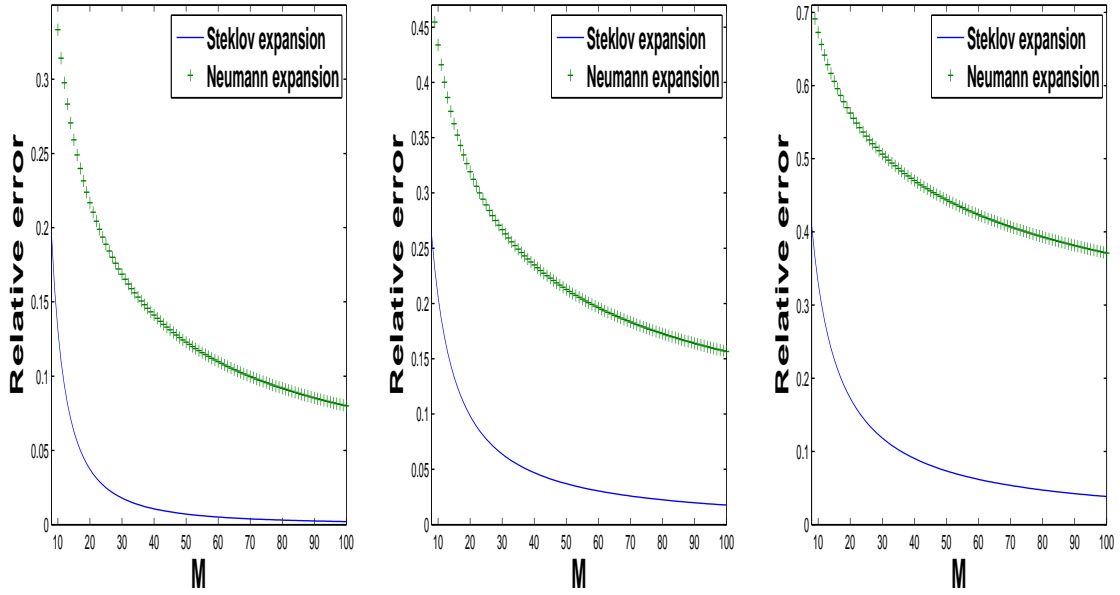


Figure 4.4: Relative errors of the M -th Steklov and Neumann approximations of f in $\|\cdot\|_2$ (left), $\|\cdot\|_\infty$ (middle), and $\|\nabla \cdot\|_2$ (right) against M .

	Relative error in $\ \cdot\ _2$		Relative error in $\ \cdot\ _\infty$		Relative error in $\ \nabla \cdot\ _2$	
	Steklov	Neumann	Steklov	Neumann	Steklov	Neumann
$M=8$	0.23532	0.33646	0.24566	0.45541	0.42959	0.66188
$M=16$	0.066016	0.2628	0.11606	0.33227	0.22477	0.61056
$M=48$	0.0076111	0.115	0.037666	0.22457	0.075806	0.43917
$M=100$	0.0017546	0.097556	0.018021	0.16661	0.036421	0.39435
α	1.81324	0.62013	1.06807	0.44281	0.93594	0.25825

Table 4.4: Relative errors of two approximations in three different norms corresponding to $M=8, 16, 48,$ and 100 and decay power α of each expansion

4.2 RELATIVE ERRORS FOR THE STEKLOV EXPANSION

(ii) Case: $h=0.8$

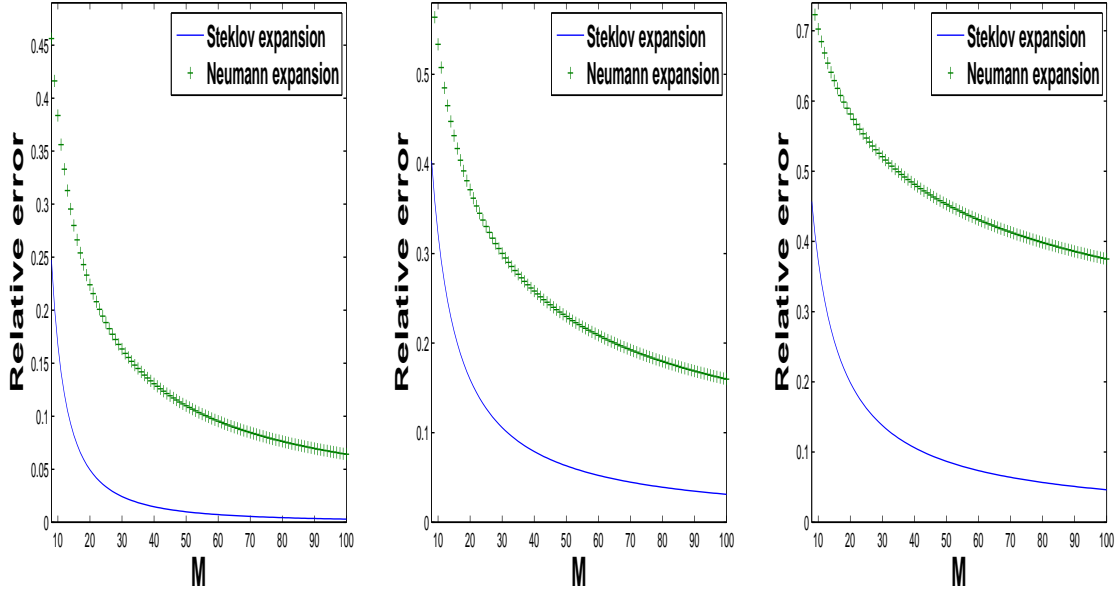


Figure 4.5: Relative errors of the M -th Steklov and Neumann approximations of f in $\|\cdot\|_2$ (left), $\|\cdot\|_\infty$ (middle), and $\|\nabla \cdot\|_2$ (right) against M .

	Relative error in $\ \cdot\ _2$		Relative error in $\ \cdot\ _\infty$		Relative error in $\ \nabla \cdot\ _2$	
	Steklov	Neumann	Steklov	Neumann	Steklov	Neumann
$M=8$	0.39048	0.48713	0.4583	0.56504	0.53293	0.72995
$M=16$	0.10549	0.30736	0.21235	0.42937	0.27599	0.64628
$M=48$	0.010813	0.10186	0.064758	0.21921	0.090487	0.44097
$M=100$	0.0025008	0.071259	0.030952	0.16696	0.043425	0.39065
α	1.1755	0.77663	1.10134	0.52389	0.90627	0.27284

Table 4.5: Relative errors of two approximations in three different norms corresponding to $M=8, 16, 48,$ and 100 and decay power α of each expansion

4.2 RELATIVE ERRORS FOR THE STEKLOV EXPANSION

(iii) Case: $h=0.5$

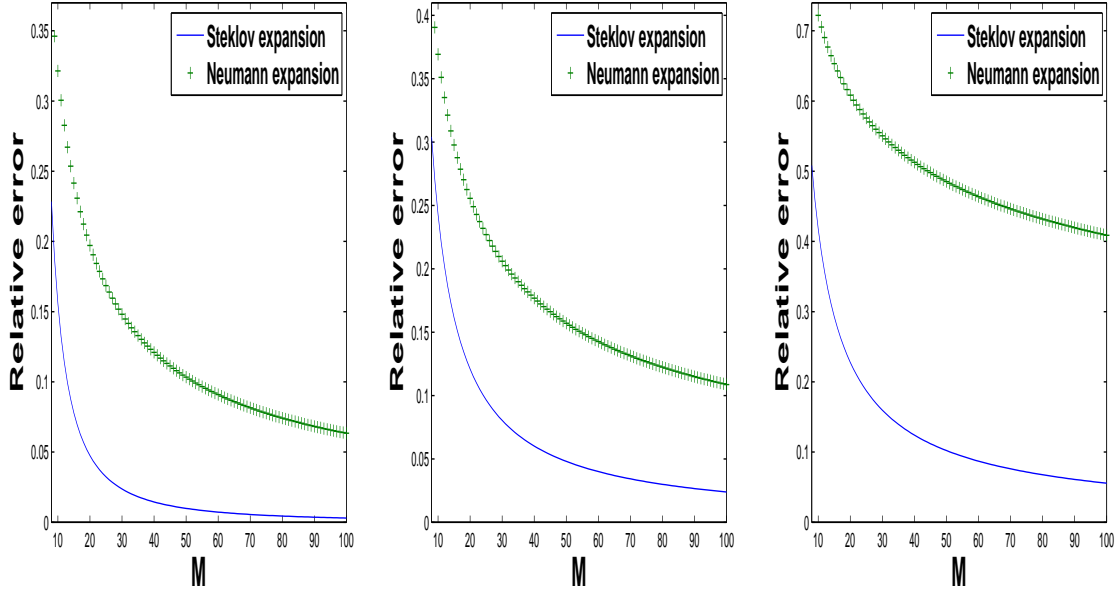


Figure 4.6: Relative errors of the Steklov expansion and the Neumann expansion of f in $\|\cdot\|_2$ (left), $\|\cdot\|_\infty$ (middle), and $\|\nabla \cdot\|_2$ (right) against M .

	Relative error in $\ \cdot\ _2$		Relative error in $\ \cdot\ _\infty$		Relative error in $\ \nabla \cdot\ _2$	
	Steklov	Neumann	Steklov	Neumann	Steklov	Neumann
$M=8$	0.2273	0.36485	0.31918	0.41866	0.50235	0.75813
$M=16$	0.089806	0.19556	0.15327	0.24876	0.31473	0.61087
$M=48$	0.010614	0.094018	0.048661	0.14528	0.10553	0.47617
$M=100$	0.0025661	0.075623	0.023901	0.12782	0.050653	0.42735
α	1.7141	0.70509	1.0068	0.53112	0.87572	0.24712

Table 4.6: Relative errors of two approximations in three different norms corresponding to $M=8, 16, 48,$ and 100 and decay power α of each expansion

4.2 RELATIVE ERRORS FOR THE STEKLOV EXPANSION

3. $f_3(x, y) := e^x \cos(y)$

(i) Case: $h=1$

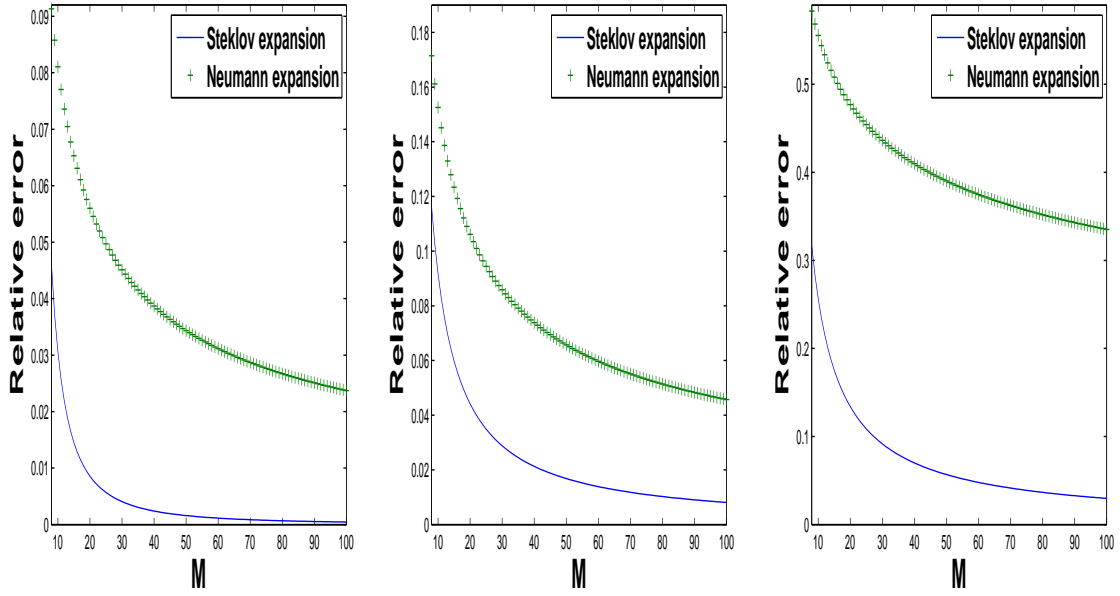


Figure 4.7: Relative errors of the M -th Steklov and Neumann approximations of f in $\|\cdot\|_2$ (left), $\|\cdot\|_\infty$ (middle), and $\|\nabla \cdot\|_2$ (right) against M .

	Relative error in $\ \cdot\ _2$		Relative error in $\ \cdot\ _\infty$		Relative error in $\ \nabla \cdot\ _2$	
	Steklov	Neumann	Steklov	Neumann	Steklov	Neumann
$M=8$	0.031515	0.090918	0.087062	0.18943	0.17451	0.56524
$M=16$	0.0085158	0.036242	0.039163	0.099367	0.089113	0.31523
$M=48$	$9.7296e^{-4}$	0.032847	0.012568	0.042084	0.029905	0.28779
$M=100$	$2.2543e^{-4}$	0.031514	0.0060059	0.036215	0.014364	0.26985
α	1.8378	0.5337	1.0545	0.52328	0.93684	0.21941

Table 4.7: Relative errors of two approximations in three different norms corresponding to $M=8, 16, 48,$ and 100 and decay power α of each expansion

4.2 RELATIVE ERRORS FOR THE STEKLOV EXPANSION

(ii) Case: $h=0.8$

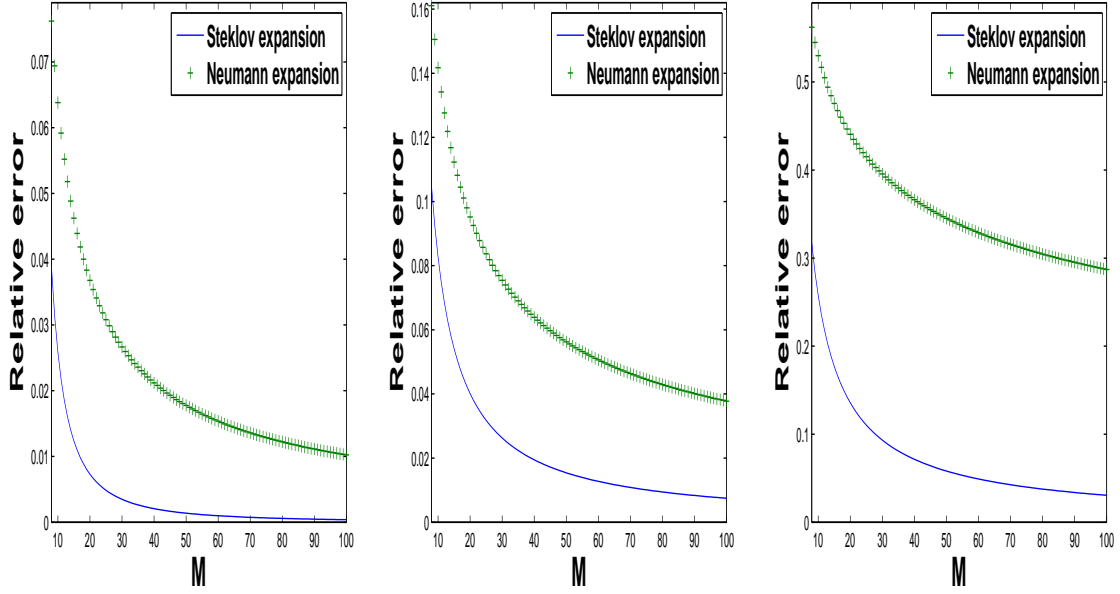


Figure 4.8: Relative errors of the M -th Steklov and Neumann approximations of f in $\|\cdot\|_2$ (left), $\|\cdot\|_\infty$ (middle), and $\|\nabla \cdot\|_2$ (right) against M .

	Relative error in $\ \cdot\ _2$		Relative error in $\ \cdot\ _\infty$		Relative error in $\ \nabla \cdot\ _2$	
	Steklov	Neumann	Steklov	Neumann	Steklov	Neumann
$M=8$	0.043536	0.078954	0.090734	0.16864	0.31844	0.58594
$M=16$	0.012631	0.044691	0.046694	0.1064	0.17249	0.47203
$M=48$	0.0015617	0.015963	0.016238	0.050817	0.061894	0.33343
$M=100$	$3.4074e^{-4}$	0.012471	0.0075501	0.044924	0.028865	0.30627
α	1.8241	0.69704	1.0483	0.49437	0.92487	0.23541

Table 4.8: Relative errors of two approximations in three different norms corresponding to $M=8, 16, 48,$ and 100 and decay power α of each expansion

4.2 RELATIVE ERRORS FOR THE STEKLOV EXPANSION

(iii) Case: $h=0.5$

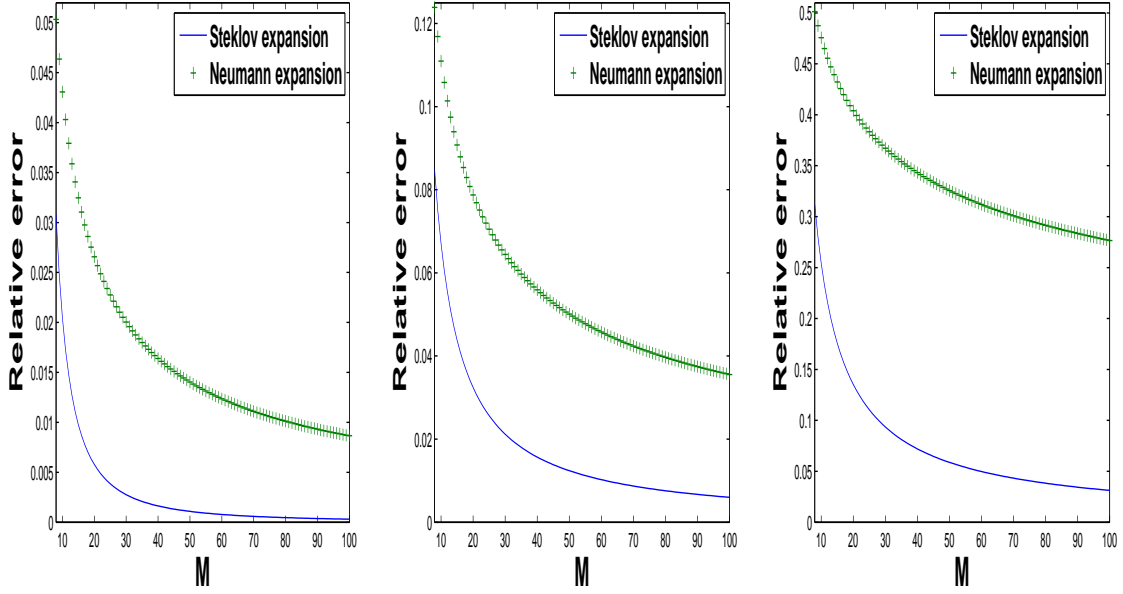


Figure 4.9: Relative errors of the M -th Steklov and Neumann approximations of f in $\|\cdot\|_2$ (left), $\|\cdot\|_\infty$ (middle), and $\|\nabla \cdot\|_2$ (right) against M .

	Relative error in $\ \cdot\ _2$		Relative error in $\ \cdot\ _\infty$		Relative error in $\ \nabla \cdot\ _2$	
	Steklov	Neumann	Steklov	Neumann	Steklov	Neumann
$M=8$	0.029402	0.060554	0.08137	0.14831	0.31304	0.53662
$M=16$	0.010927	0.026931	0.041328	0.07982	0.18936	0.40797
$M=48$	0.0011222	0.012298	0.012354	0.045946	0.059625	0.3139
$M=100$	$2.8045e^{-4}$	0.011414	0.0061766	0.043488	0.029283	0.30064
α	1.8241	0.69698	1.0483	0.4943	0.91009	0.23537

Table 4.9: Relative errors of two approximations in three different norms corresponding to $M=8, 16, 48,$ and 100 and decay power α of each expansion

4.2 RELATIVE ERRORS FOR THE STEKLOV EXPANSION

In our experiments, we analyze relative errors of two different expansions of three harmonic functions, $x^2 - y^2$, $x^3 - 3xy^2$, and $e^x \cos(y)$, respectively. The results are plotted in Figures (4.1)-(4.9). Each figure has the x-axis and the y-axis which represent the number of terms in expansions and relative error, respectively. These results clearly show that the Neumann expansion converges very slowly whereas the Steklov expansion can quickly reconstruct a function. In three different norms, fewer terms are necessary for the Steklov expansion to converge compared to the Neumann expansion. Figures also show good L^2 -convergence while the convergence in other two norms is less favorable.

Similar conclusions can be drawn from Tables (4.1)-(4.9), which report each relative error corresponding to $M=8, 16, 48$, and 100 and each decay power in three different norms. The decay power allows us to estimate the rate of convergence for each approximation.

Table (4.10) shows that how many terms are required to reduce each relative error of the Steklov and Neumann expansion of f_1, f_2 , and f_3 as defined above to $\epsilon = 0.05$, respectively.

	Relative error in $\ \cdot\ _2$		Relative error in $\ \cdot\ _\infty$		Relative error in $\ \nabla \cdot\ _2$	
	Steklov	Neumann	Steklov	Neumann	Steklov	Neumann
$f_1(x, y)$	4	12	7	55	24	over 500
$f_2(x, y)$	13	180	44	226	73	over 500
$f_3(x, y)$	8	17	16	120	56	over 500

Table 4.10: The number of terms in expansions such that relative errors reach to $\epsilon = 0.05$ corresponding to f_i for $1 \leq i \leq 3$ for the case when $h = 1$

The Neumann eigenvalues and eigenfunctions have been used to represent functions as the traditional spectral representation. But as long as the function is harmonic, the Steklov expansion is a competitor of this traditional one since the Steklov

4.2 RELATIVE ERRORS FOR THE STEKLOV EXPANSION

expansion does not suffer from the number of eigenfunction terms to converge to a fixed accuracy. Hence, the Steklov spectral expansion is a promising alternative for representing harmonic functions.

Chapter 5

Solutions of Boundary Value Problems on Ω

5.1 The Harmonic Dirichlet Problem

We consider a function $u \in H^1(\Omega)$ satisfies

$$\Delta u = 0 \quad \text{in } \Omega \tag{5.1}$$

$$u = \eta \quad \text{on } \partial\Omega \tag{5.2}$$

This is often known as the *Harmonic Dirichlet* (HD) problem. There are various different theories for solving the HD problem on Ω . See the comprehensive survey by Benilan in Chapter 2 of [9] and also the lectures of Kenig [13].

The description of trace spaces using Steklov eigenfunctions is developed in [2] and its application to Dirichlet problems for harmonic functions is described in Chapter 6 of [4]. Our interest is in finding solutions of this problem when η is continuous on the

5.1 THE HARMONIC DIRICHLET PROBLEM

boundary. When η is not continuous on the boundary, especially not in $H^{\frac{1}{2}}(\partial\Omega)$ (see Chapter 4 and 6 of [5]), the generalized harmonic Dirichlet problem that arises in the theory of thin films is described in Chapter 5 of [3].

Here we assume that $\eta = \Gamma u \in L^2(\partial\Omega, d\sigma)$ and $\Omega = [-L, L] \times [-Lh, Lh]$. We consider approximations of the solution of the HD problem on Ω in terms of the harmonic Steklov eigenfunctions.

Theorem 4.2 implies that the solution of the HD problem may be represented by

$$u(x, y) = \sum_{i=0}^{\infty} \eta_i \hat{s}_i(x, y) \text{ for } (x, y) \in \bar{\Omega} \text{ with } \eta_i := \langle \eta, \hat{s}_i \rangle_{2, \partial\Omega} \quad (5.3)$$

and we expect the partial sums $u_M(x, y) = \sum_{i=0}^M \eta_i \hat{s}_i(x, y)$ for $(x, y) \in \bar{\Omega}$ to be good approximations of the solution. Clearly, each partial sum is harmonic and has a continuous trace η on the boundary. As observed in the previous chapter, the finite sum of the Steklov expansion of u can approximate the solution of the HD problem under a small error. Define the Steklov approximation of u to be the M -th partial sum of this expansion and denoted by u_M . When the solution is obtained approximately by u_M , there could be a couple of advantages of using the Steklov expansion for the HD problem. As described in the preceding chapter, u_M can quickly reconstruct the solution of the HD problem. The fact that the number of Steklov eigenfunction expected to use is small yields that computational costs may be saved when the Steklov expansion method is implemented on Matlab.

Moreover, the Steklov expansion only requires evaluating boundary integrals. Once boundary normalized Steklov eigenfunctions are known, as described in Section 3.6, the set of the eigenfunctions spans $L^2(\partial\Omega, d\sigma)$. The boundary condition of

5.1 THE HARMONIC DIRICHLET PROBLEM

the HD problem is well approximated by the Steklov expansion. Here we provide numerical experiments and reveal these advantages.

Assume η is continuous and bounded on $\partial\Omega$ and we will look at functions that are even or odd about the center of each side. The HD problem on $\Omega = [-1, 1] \times [-1, 1]$ is solved by using the Steklov expansion method. We do not know the exact solution of the problem, but we perform experiments for u_M corresponding to $M=8, 16, 48,$ and 100 . Figures and contour sets of u_M in $\bar{\Omega}$ are provided.

5.1 THE HARMONIC DIRICHLET PROBLEM

1.

$$\eta_1(x, y) = \begin{cases} 1 - x^2 & \text{on } \Gamma_1 \text{ and } \Gamma_3 \\ 1 - y^2 & \text{on } \Gamma_2 \text{ and } \Gamma_4 \end{cases}$$

This $\eta_1(x, y)$ is a piecewise function that is even about the center on each side, non negative on $\partial\Omega$, and $\bar{\eta}_1 = \frac{2}{3} > 0$. Figure (5.1) shows graphs of $u_M(x, y)$ in $\bar{\Omega}$ and next Figure (5.2) represents contour lines of $u_M(x, y)$ corresponding to $M=8, 16, 48,$ and $100,$ respectively.

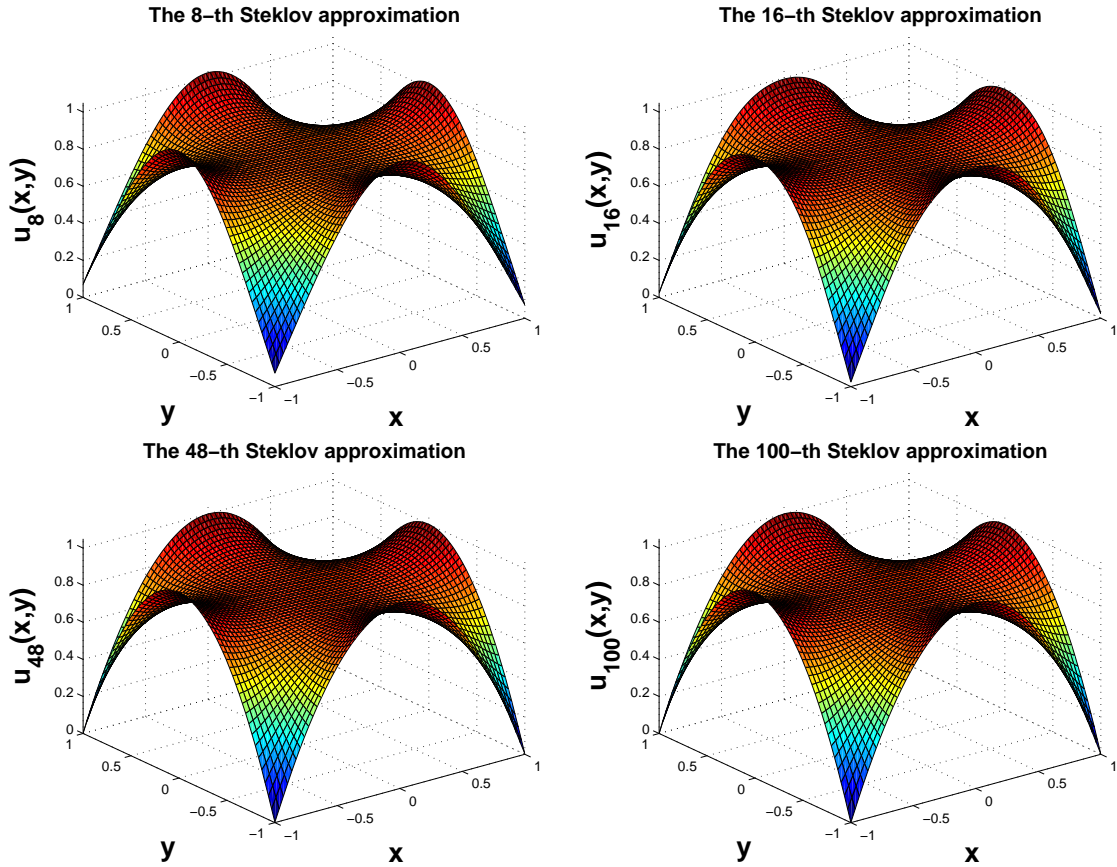


Figure 5.1: The M -th Steklov approximations of the HD Problem on $[-1, 1] \times [-1, 1]$ for $\eta = \eta_1$ corresponding to $M=8$ (Left top), 16 (Right top), 48 (Left bottom), and 100 (Right bottom).

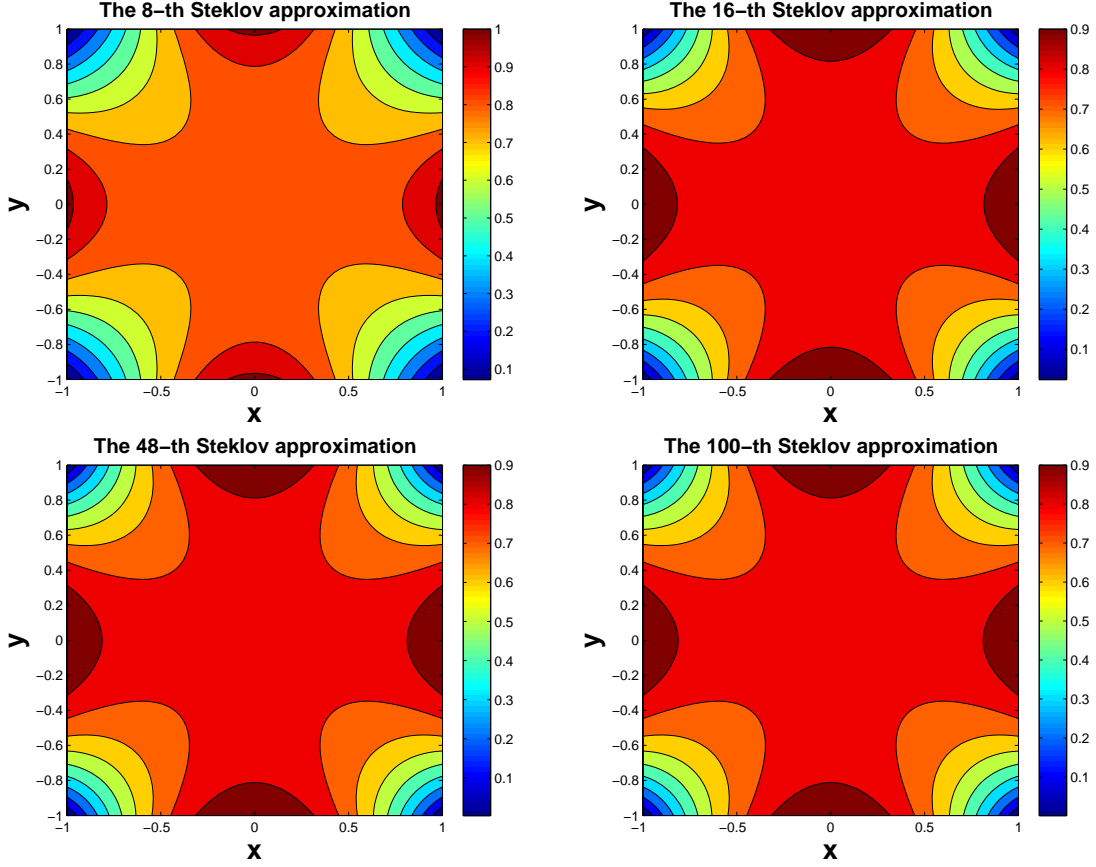


Figure 5.2: Contour plots of the M -th Steklov approximations of the HD Problem on $[-1, 1] \times [-1, 1]$ for $\eta = \eta_1$ corresponding to $M=8$ (Left top), 16 (Right top), 48 (Left bottom), and 100 (Right bottom).

We observe that for each M , $u_M(x, y)$ is symmetric about both x -axis and y -axis, non negative on $\partial\Omega$ and $\overline{u_M} = \frac{2}{3}$. In Figure (5.2), we see that if (x, y) is the center of Ω , then u_M is quite flat. We point out that there is no significant difference between $u_M(x, y)$ against M for $(x, y) \in \overline{\Omega}$ for $M \geq 16$ and

$\max_{(x,y) \in \partial\Omega} |\eta_1(x, y) - u_{100}(x, y)| = 8.5826e^{-4}$. Hence a solution \tilde{u} of the HD problem on $\Omega = [-1, 1] \times [-1, 1]$ where $\eta = \eta_1$ from the maximum principles(see Section 8.3 of [19]) obeys $|\tilde{u}(x, y) - u_{100}(x, y)| \leq 8.5826e^{-4}$ for all $(x, y) \in \overline{\Omega}$.

5.1 THE HARMONIC DIRICHLET PROBLEM

2.

$$\eta_2(x, y) = \begin{cases} 1 - x^3 & \text{on } \Gamma_1 \\ 1 + y^3 & \text{on } \Gamma_2 \\ 1 + x^3 & \text{on } \Gamma_3 \\ 1 - y^3 & \text{on } \Gamma_4 \end{cases}$$

This $\eta_2(x, y)$ is a continuous function that is odd about the center on each side, non negative, and $\overline{\eta_2} = 1 > 0$.

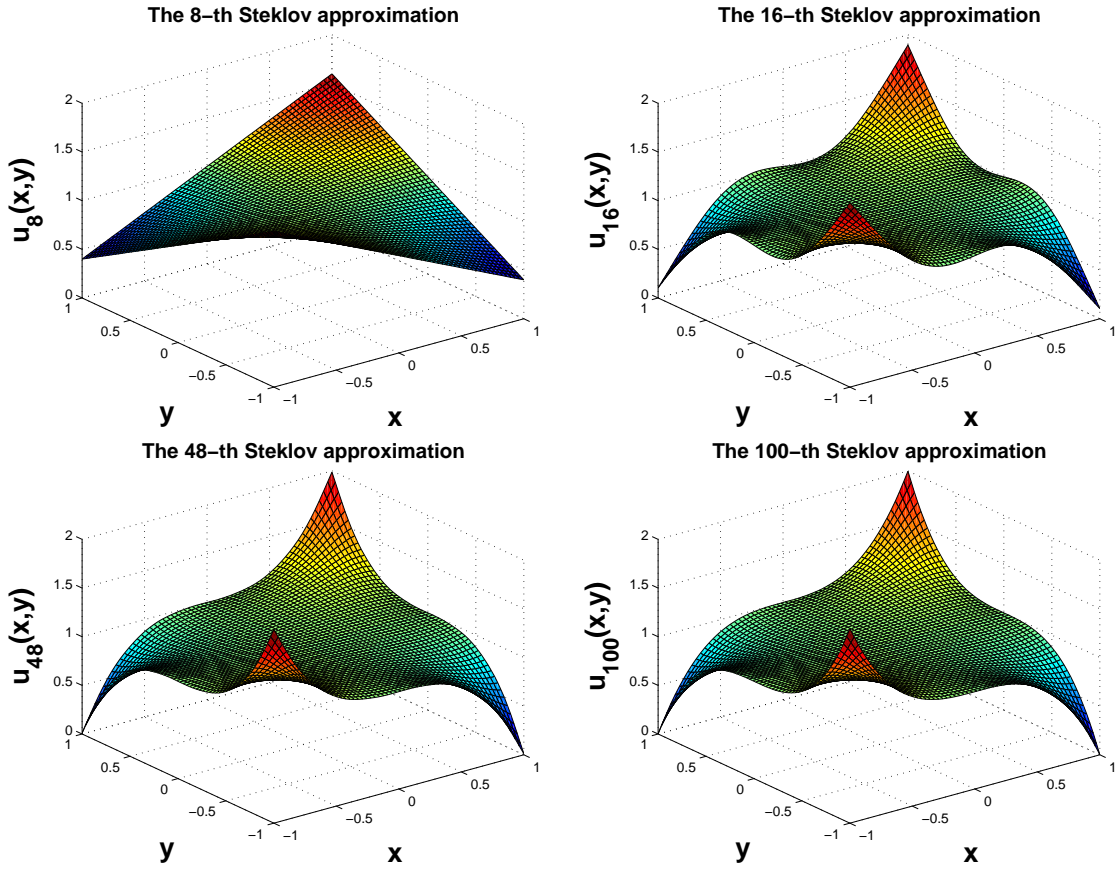


Figure 5.3: The M-th Steklov approximations of the HD Problem on $[-1, 1] \times [-1, 1]$ for $\eta = \eta_2$ corresponding to $M=8$ (Left top), 16 (Right top), 48 (Left bottom), and 100 (Right bottom).

5.1 THE HARMONIC DIRICHLET PROBLEM

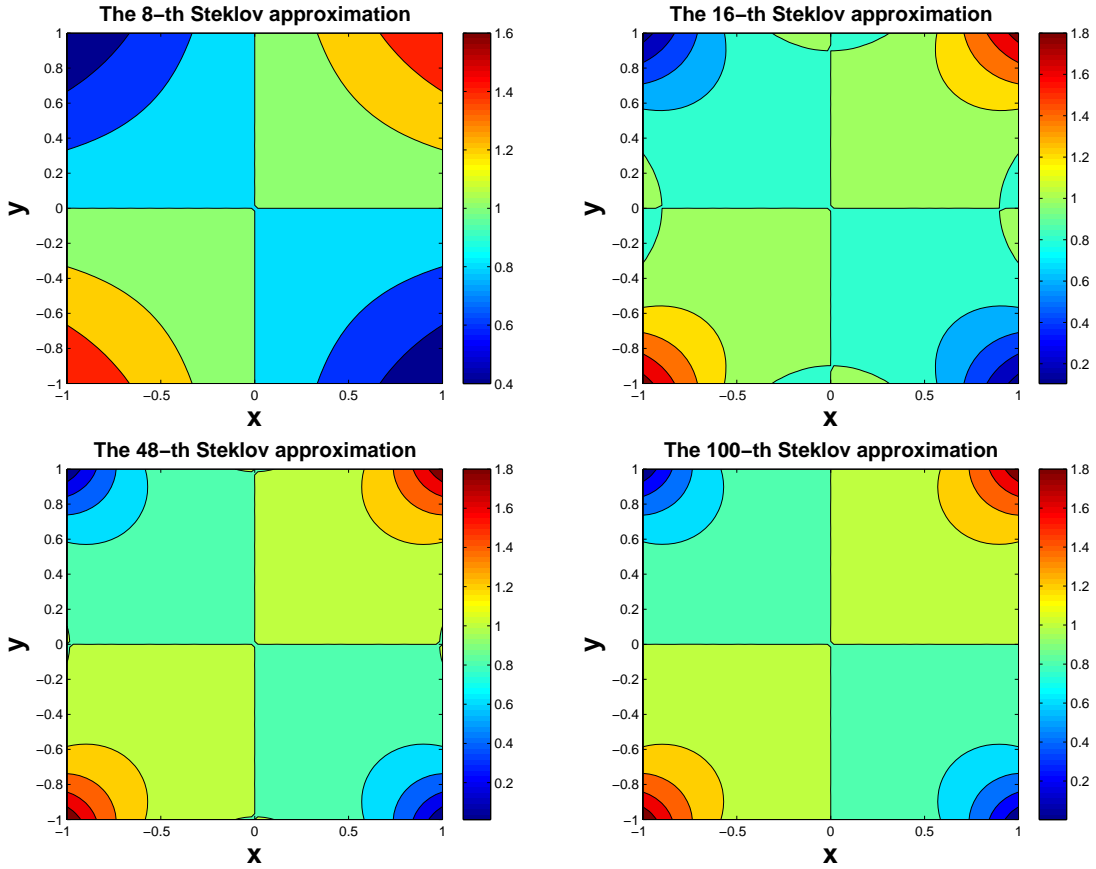


Figure 5.4: Contour plots of the M -th Steklov approximations of the HD Problem on $[-1, 1] \times [-1, 1]$ for $\eta = \eta_2$ corresponding to $M=8$ (Left top), 16 (Right top), 48 (Left bottom), and 100 (Right bottom).

Figure (5.3) shows that on each side u_8 is linearly piecewise while η_2 is cubic on each side. So the 8-th partial sum, u_8 is not a very good approximation to the solution of the HD problem on $\Omega = [-1, 1] \times [-1, 1]$ for $\eta = \eta_2$. However, we see that each u_M is a cubic function that is odd about the center on each side similar to η_2 and $\overline{u_M} = 1$ for $M=16, 48, \text{ and } 100$. Especially, $\max_{(x,y) \in \partial\Omega} |\eta_2(x,y) - u_{100}(x,y)| = 0.0023938$. Hence we can say that a solution \tilde{u} of this problem obeys $|\tilde{u}(x,y) - u_{100}(x,y)| \leq 0.0023938$ for all $(x,y) \in \overline{\Omega}$.

5.1 THE HARMONIC DIRICHLET PROBLEM

3.

$$\eta_3(x, y) = \begin{cases} \cos(4\pi x) & \text{on } \Gamma_1 \text{ and } \Gamma_3 \\ \cos(2\pi y) & \text{on } \Gamma_2 \text{ and } \Gamma_4 \end{cases}$$

This $\eta_3(x, y)$ is a piecewise function that is even about zero on each side and $\overline{\eta_3} = 0$. Compared against η_1 , this function involves more oscillations on each side. Especially, there are lots of oscillations on Γ_1 and Γ_3 .

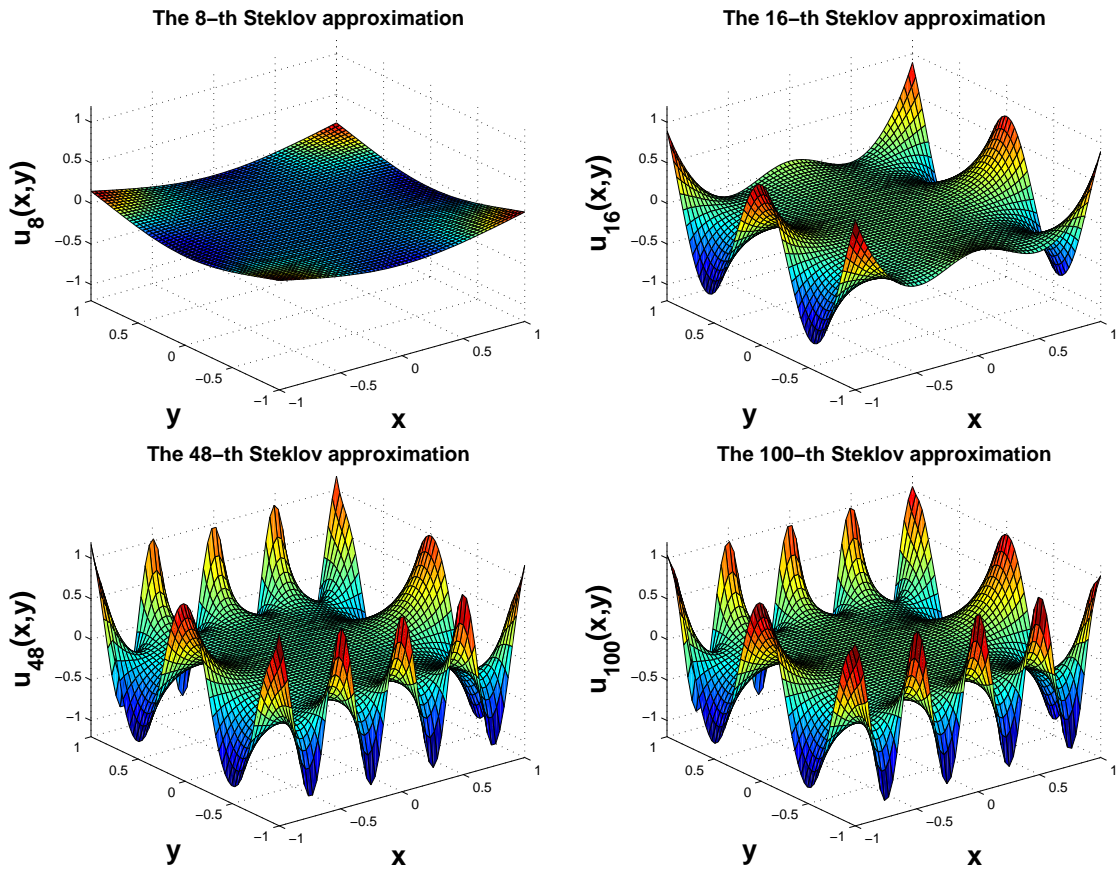


Figure 5.5: The M -th Steklov approximations of the HD Problem on $[-1, 1] \times [-1, 1]$ for $\eta = \eta_3$ corresponding to $M=8$ (Left top), 16 (Right top), 48 (Left bottom), and 100 (Right bottom).

5.1 THE HARMONIC DIRICHLET PROBLEM

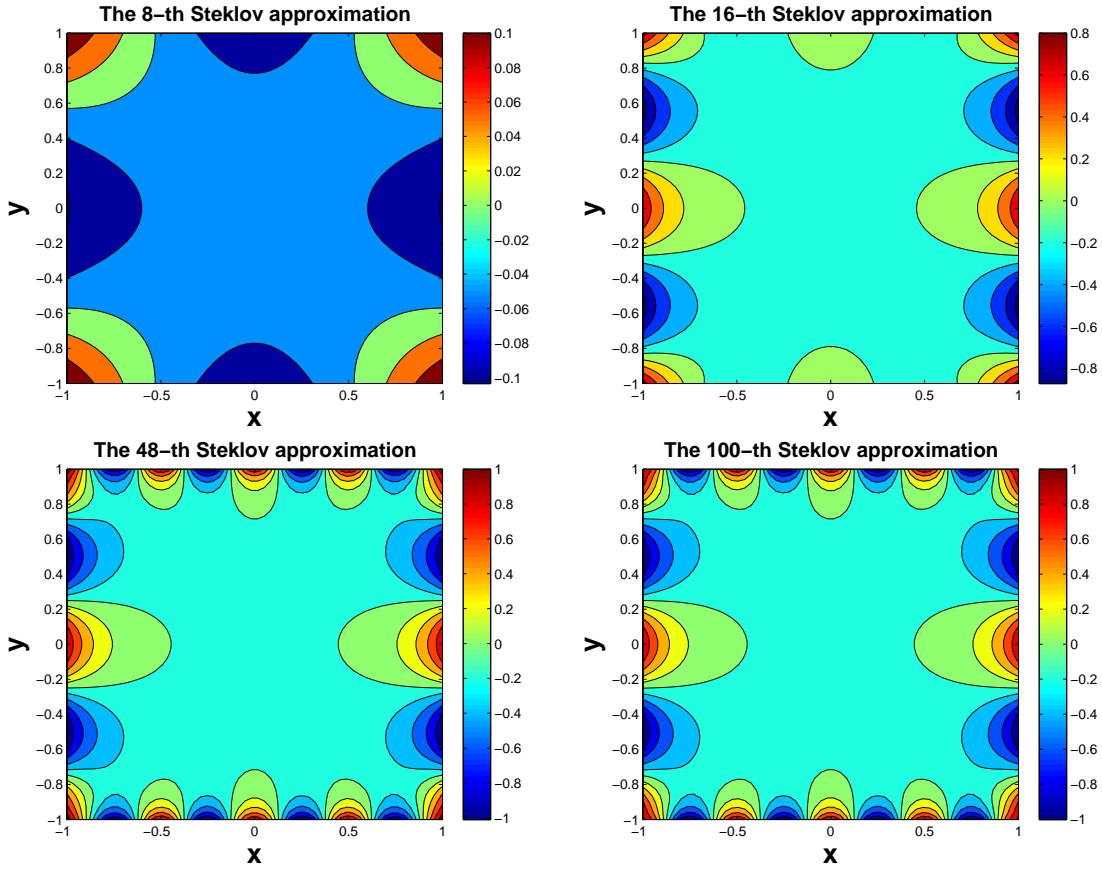


Figure 5.6: Contour plots of the M -th Steklov approximations of the HD Problem on $[-1, 1] \times [-1, 1]$ for $\eta = \eta_3$ corresponding to $M=8$ (Left top), 16 (Right top), 48 (Left bottom), and 100 (Right bottom).

Figure (5.6) shows that for each M , u_M is symmetric about both x -axis and y -axis and around the center, it is flat. In Figure (5.5), we see that nice approximation u_M are not obtained for $M \leq 16$ since there are fewer oscillations on each side than in η_3 . However, u_{48} is oscillating as much as η_3 and $\overline{u_{48}} = 6.2153e^{-14}$. We point out that $\max_{(x,y) \in \partial\Omega} |\eta_3(x,y) - u_{100}(x,y)| = 0.0042578$. Hence the Steklov expansion method gives a good approximation of a solution of the HD Problem on $\Omega = [-1, 1] \times [-1, 1]$ for $\eta = \eta_3$.

5.2 The Harmonic Neumann Problem

In this section ,we want to approximate solutions $u \in H^1_{\partial}(\Omega)$ of

$$\Delta u = 0 \quad \text{in } \Omega \quad (5.4)$$

$$D_{\nu}u = \eta \quad \text{on } \partial\Omega \quad (5.5)$$

Here $\eta \in L^2(\partial\Omega, d\sigma)$. This problem will be called the *Harmonic Neumann* (HN) problem. The weak form of (5.4)-(5.5) is to find a function u in $H^1(\Omega)$ satisfying

$$\int_{\Omega} \nabla n \cdot \nabla v \, dx = \delta \int_{\partial\Omega} n v \, d\sigma \quad \text{for all } v \in H^1(\Omega) \quad (5.6)$$

Since $\mathcal{S} = \{\hat{s}_i : i \geq 0\}$ is a orthogonal basis of $\mathcal{H}(\Omega)$, we can represent a solution of this problem by $u(x, y) = \sum_{i=0}^{\infty} c_i \hat{s}_i(x, y)$ on Ω for non zero constant $c_i, i \geq 0$. Then the boundary condition is that

$$D_{\nu}u(x, y) = \sum_{i=0}^{\infty} c_j D_{\nu} \hat{s}_i(x, y) \quad (5.7)$$

$$= \sum_{i=0}^{\infty} c_i \delta_i \hat{s}_i(x, y) \quad (5.8)$$

The second equality holds from (3.2). One has

$$\eta(x, y) = \sum_{i=0}^{\infty} \langle \eta, \hat{s}_i \rangle_{2, \partial\Omega} \hat{s}_i(x, y) \quad \text{for } (x, y) \in \partial\Omega \quad (5.9)$$

Comparing with (5.8) yields that $c_i \delta_i = \langle \eta, \hat{s}_i \rangle_{2, \partial\Omega}$. Equivalently

$$c_i = \frac{\langle \eta, \hat{s}_i \rangle_{2, \partial\Omega}}{\delta_i} \quad \text{for } i > 0 \quad (5.10)$$

5.2 THE HARMONIC NEUMANN PROBLEM

Put $v(x) \equiv 1$ on $\bar{\Omega}$ and substitute on (5.6), then a necessary condition for the HN problem to have a solution is that

$$\int_{\partial\Omega} \eta \, d\sigma = 0 \quad (5.11)$$

It implies that $c_0 = 0$. In this case, Theorem 9.3 of [1] says that this problem has a unique solution. Then the unique solution of the HN problem has the representation

$$u(x, y) = \sum_{i=1}^{\infty} \frac{\langle \eta, \hat{s}_i \rangle_{2, \partial\Omega}}{\delta_i} \hat{s}_i(x, y) \text{ for } (x, y) \in \bar{\Omega} \quad (5.12)$$

We recall η_3 from the preceding section. Since $\bar{\eta}_3 = 0$, there exists a unique solution of the HN problem on Ω for $\eta = \eta_3$. We provide similar numerical results of the Steklov approximations of a solution of the HN problem on $\Omega = [-1, 1] \times [-1, 1]$ where $\eta = \eta_3$ as performed in the previous section.

5.2 THE HARMONIC NEUMANN PROBLEM

$$\eta_3(x, y) = \begin{cases} \cos(4\pi x) & \text{on } \Gamma_1 \text{ and } \Gamma_3 \\ \cos(2\pi y) & \text{on } \Gamma_2 \text{ and } \Gamma_4 \end{cases}$$

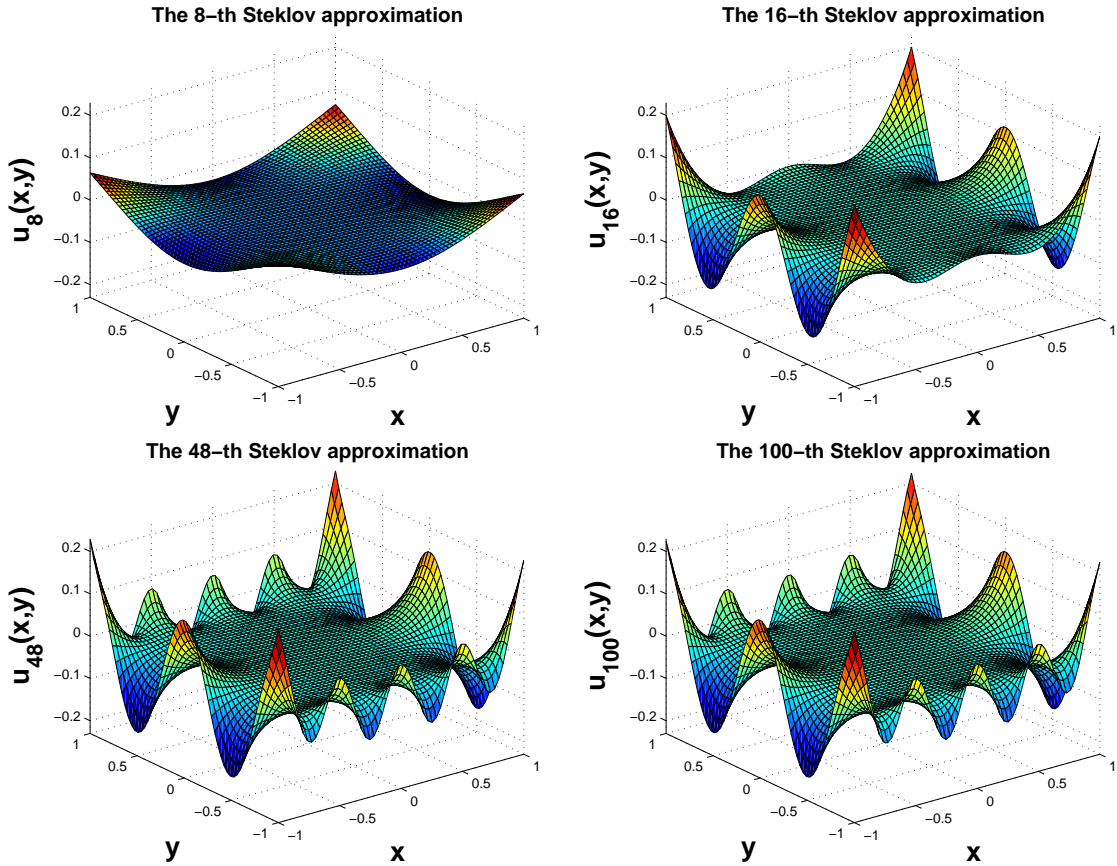


Figure 5.7: The M-th Steklov approximations of the HN Problem on $[-1, 1] \times [-1, 1]$ for $\eta = \eta_3$ corresponding to $M=8$ (Left top), 16(Right top), 48(Left bottom), and 100(Right bottom).

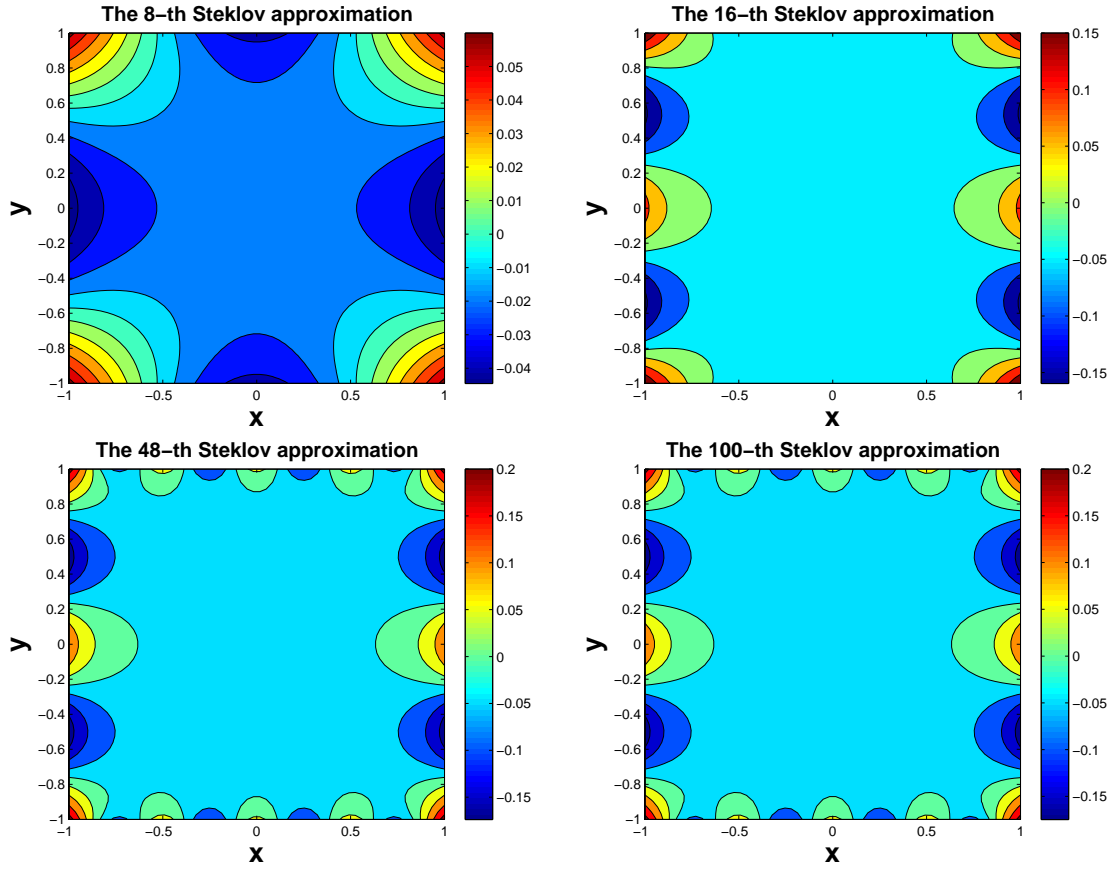


Figure 5.8: Contour plots of the M -th Steklov approximations of the HN Problem on $[-1, 1] \times [-1, 1]$ for $\eta = \eta_3$ corresponding to $M=8$ (Left top), 16 (Right top), 48 (Left bottom), and 100 (Right bottom).

5.3 The Harmonic Robin Problem

In this section, we consider a function $u \in H^1(\Omega)$ satisfies

$$\Delta u = 0 \quad \text{in } \Omega \quad (5.13)$$

$$D_\nu u + u = \eta \quad \text{on } \partial\Omega \quad (5.14)$$

Here $\eta \in L^2(\partial\Omega, d\sigma)$. This problem will be called the *Harmonic Robin* (HR) problem.

As described in the preceding section, in order to approximate a solution of this problem we start with $u(x, y) = \sum_{i=0}^{\infty} c_i \hat{s}_i(x, y)$ on Ω for non zero constant c_i , $i \geq 0$.

Then the boundary condition becomes

$$\begin{aligned} D_\nu u(x, y) + u(x, y) &= \sum_{i=0}^{\infty} c_i D_\nu \hat{s}_i(x, y) + \sum_{i=0}^{\infty} c_i \hat{s}_i(x, y) \\ &= \sum_{i=0}^{\infty} c_i \delta_i \hat{s}_i(x, y) + \sum_{i=0}^{\infty} c_i \hat{s}_i(x, y) \\ &= \sum_{i=0}^{\infty} c_i (\delta_i + 1) \hat{s}_i(x, y) \end{aligned}$$

Comparing with (5.9) yields that

$$c_i = \frac{\langle \eta, \hat{s}_i \rangle_{2, \partial\Omega}}{\delta_i + 1} \quad \text{for } i \geq 0 \quad (5.15)$$

Hence we can represent the solution of the HR problem by

$$u(x, y) = \sum_{i=0}^{\infty} \frac{\langle \eta, \hat{s}_i \rangle_{2, \partial\Omega}}{\delta_i + 1} \hat{s}_i(x, y) \quad \text{for } (x, y) \in \bar{\Omega} \quad (5.16)$$

Again we recall η_1 , η_2 , and η_3 from Section 5.1. We perform numerical experiments

5.3 THE HARMONIC ROBIN PROBLEM

of the Steklov approximations of a solution of the HR problem on $\Omega = [-1, 1] \times [-1, 1]$.

1.

$$\eta_1(x, y) = \begin{cases} 1 - x^2 & \text{on } \Gamma_1 \text{ and } \Gamma_3 \\ 1 - y^2 & \text{on } \Gamma_2 \text{ and } \Gamma_4 \end{cases}$$

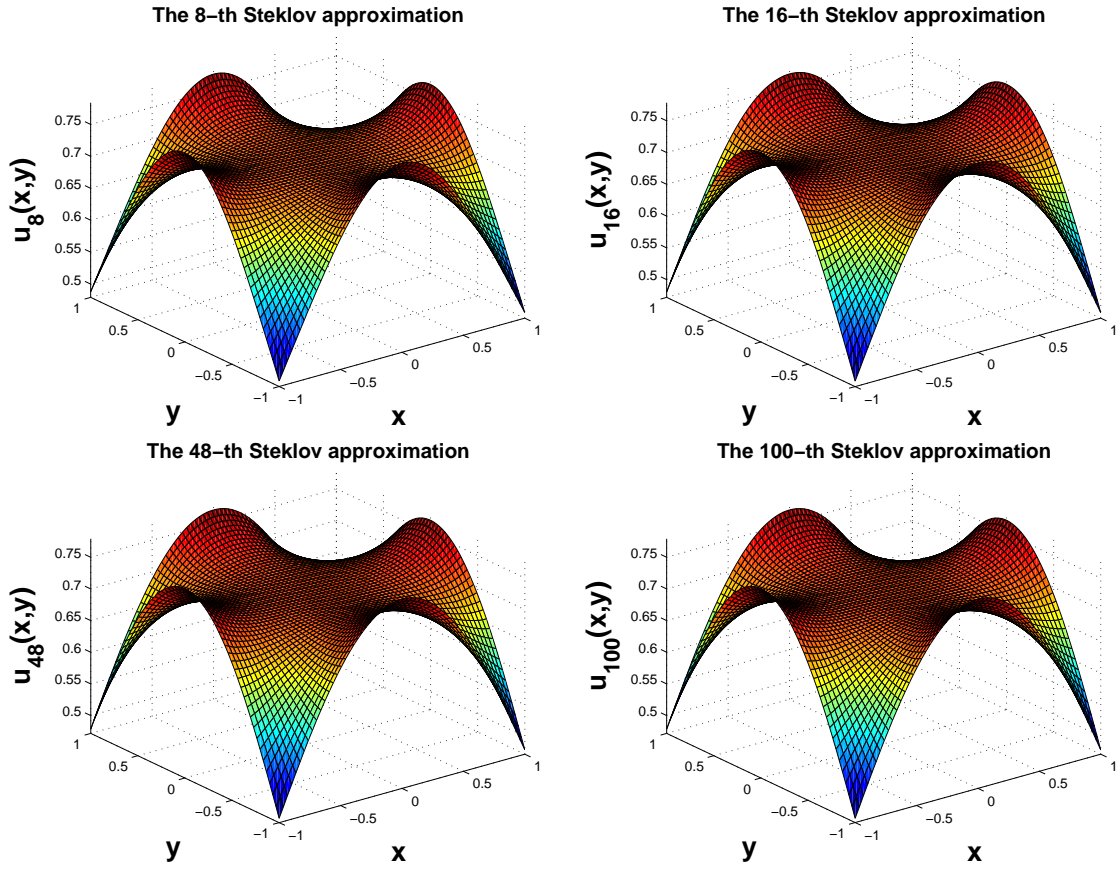


Figure 5.9: The M -th Steklov approximations of the HR Problem on $[-1, 1] \times [-1, 1]$ for $\eta = \eta_1$ corresponding to $M=8$ (Left top), 16 (Right top), 48 (Left bottom), and 100 (Right bottom).

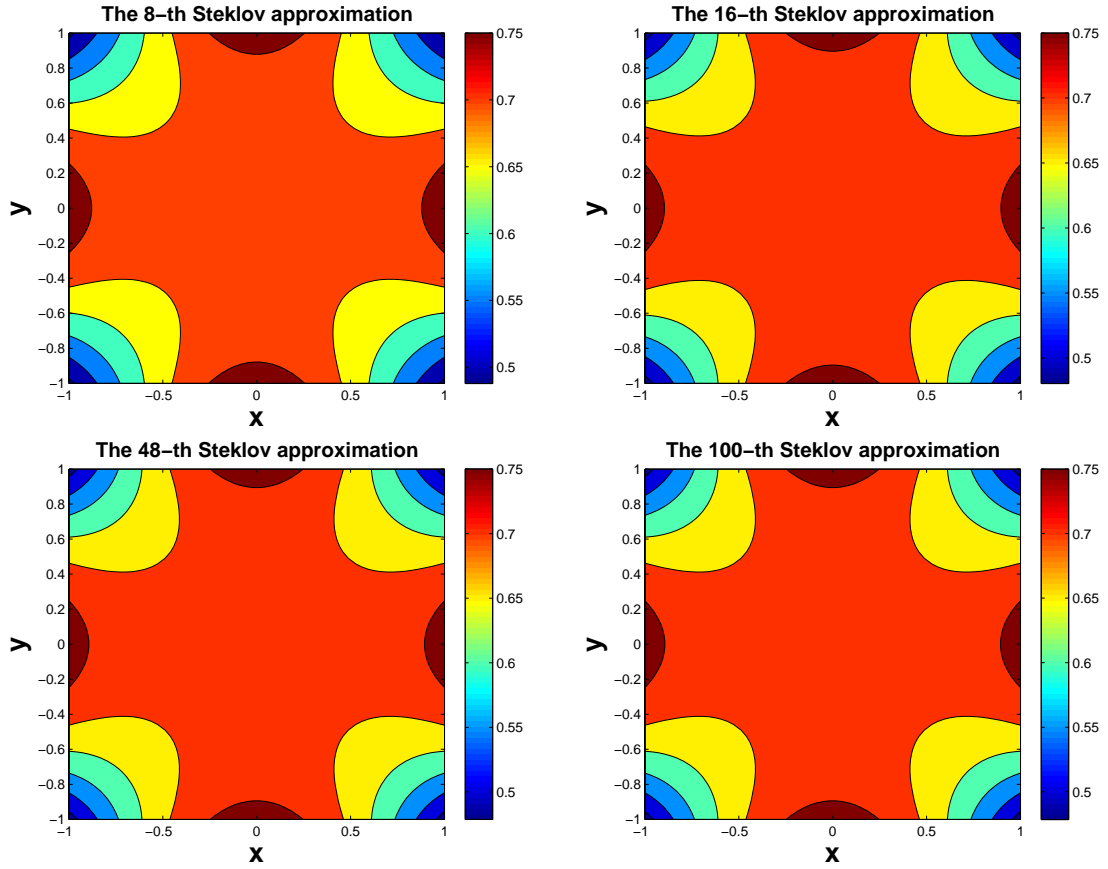


Figure 5.10: Contour lines of the M-th Steklov approximations of the HR Problem on $[-1, 1] \times [-1, 1]$ for $\eta = \eta_1$ corresponding to M=8(Left top), 16(Right top), 48(Left bottom), and 100(Right bottom).

5.3 THE HARMONIC ROBIN PROBLEM

2.

$$\eta_2(x, y) = \begin{cases} 1 - x^3 & \text{on } \Gamma_1 \\ 1 + y^3 & \text{on } \Gamma_2 \\ 1 + x^3 & \text{on } \Gamma_3 \\ 1 - y^3 & \text{on } \Gamma_4 \end{cases}$$

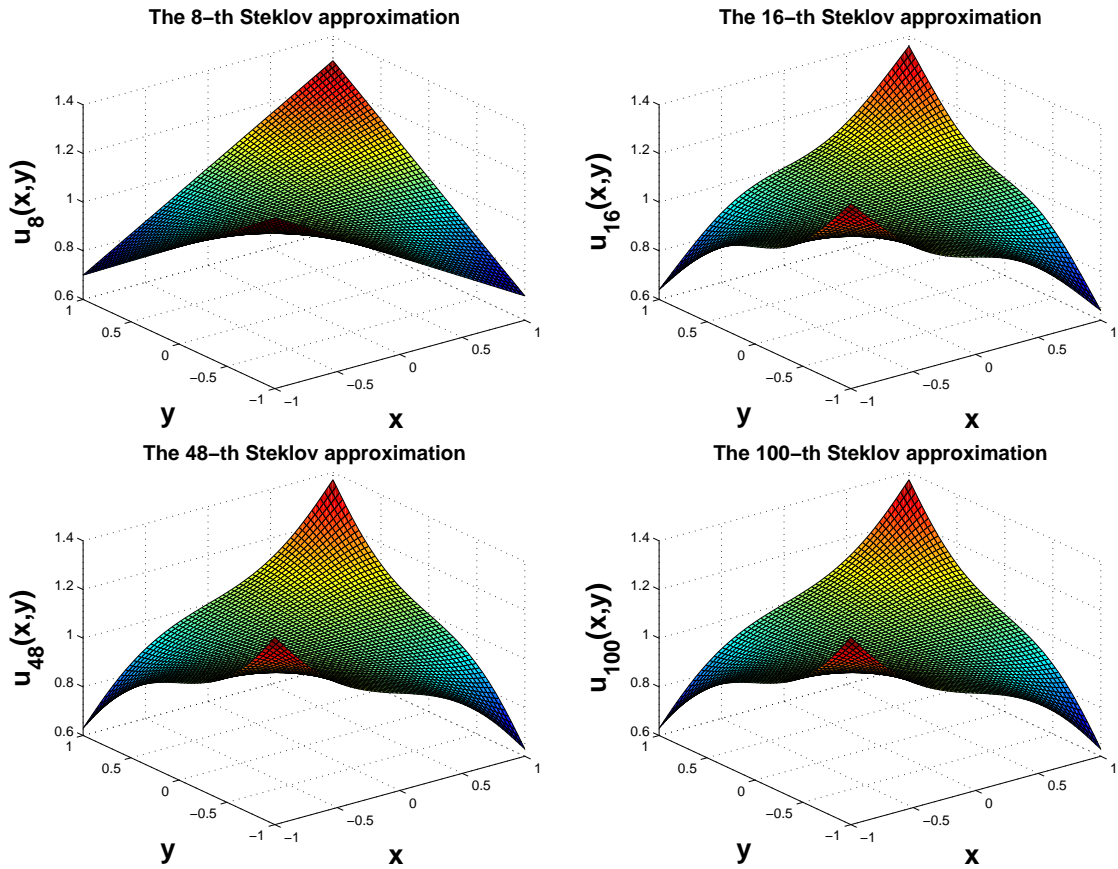


Figure 5.11: The M-th Steklov approximations of the HR Problem on $[-1, 1] \times [-1, 1]$ for $\eta = \eta_2$ corresponding to M=8(Left top), 16(Right top), 48(Left bottom), and 100(Right bottom).

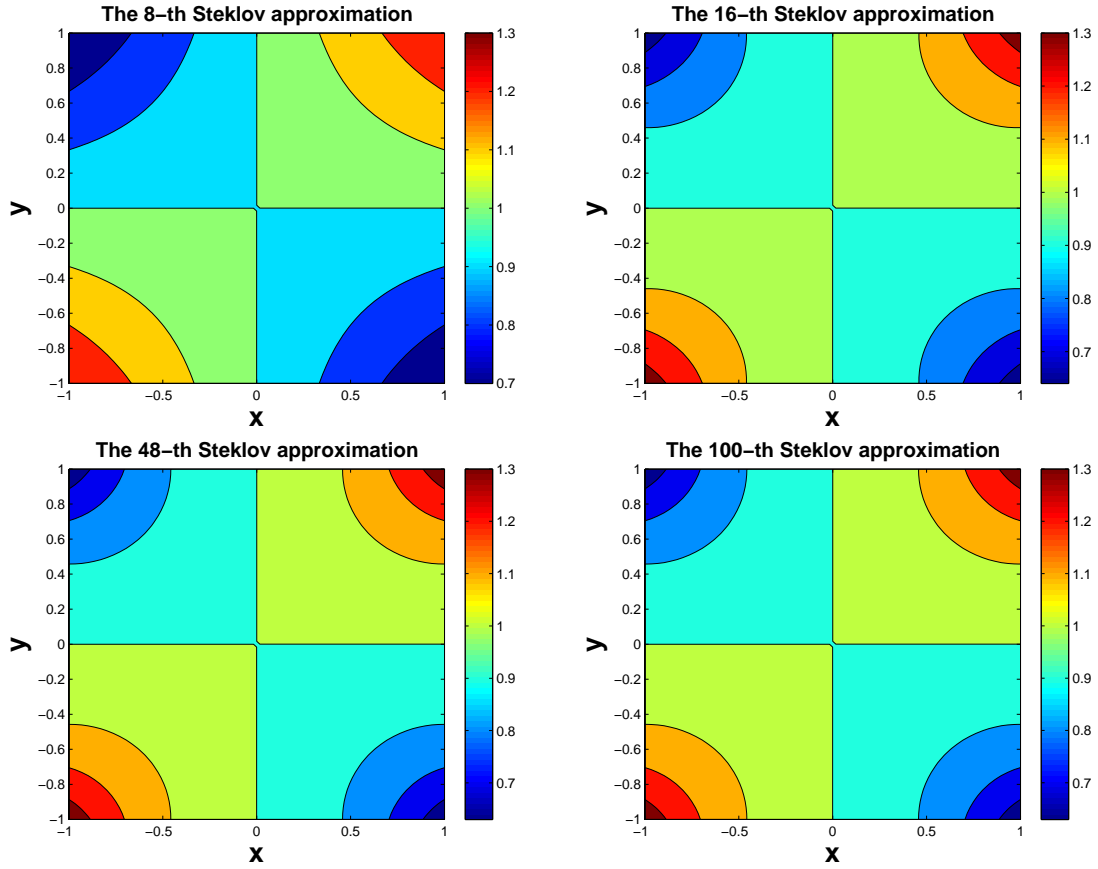


Figure 5.12: Contour lines of the M -th Steklov approximations of the HR Problem on $[-1, 1] \times [-1, 1]$ for $\eta = \eta_2$ corresponding to $M=8$ (Left top), 16 (Right top), 48 (Left bottom), and 100 (Right bottom).

5.3 THE HARMONIC ROBIN PROBLEM

3.

$$\eta_3(x, y) = \begin{cases} \cos(4\pi x) & \text{on } \Gamma_1 \text{ and } \Gamma_3 \\ \cos(2\pi y) & \text{on } \Gamma_2 \text{ and } \Gamma_4 \end{cases}$$

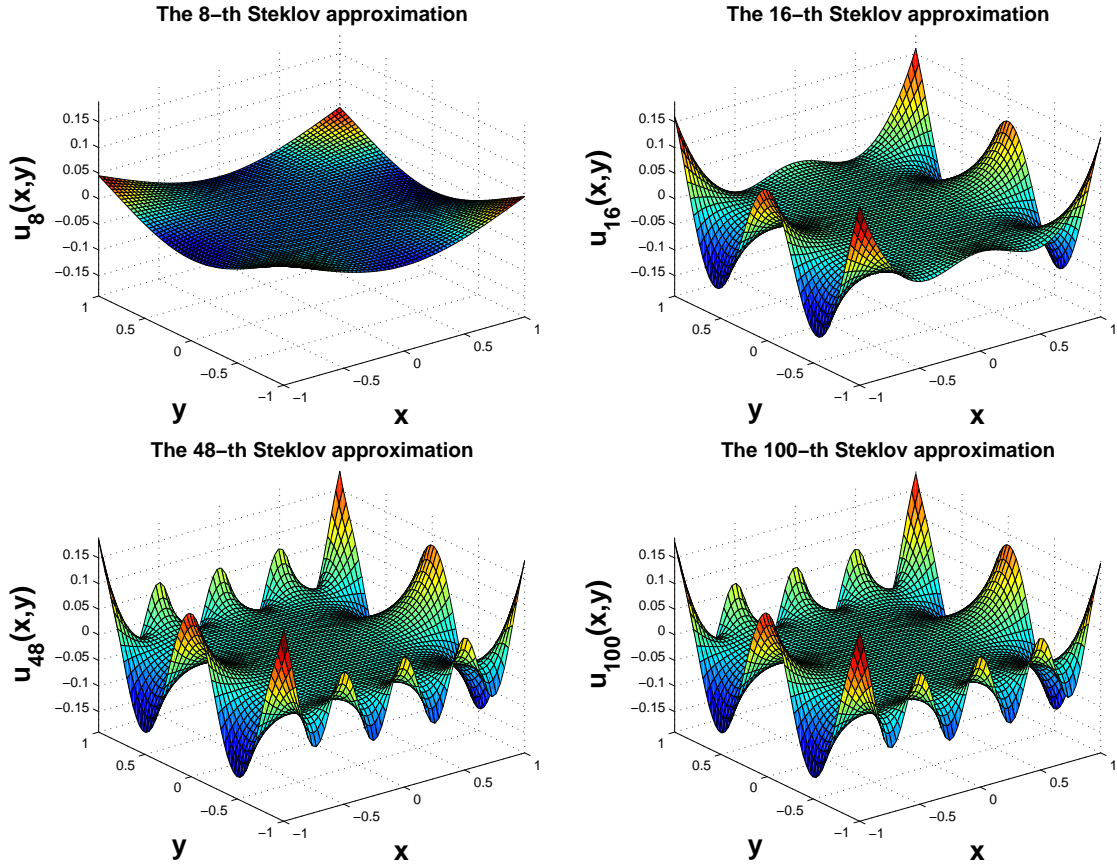


Figure 5.13: The M-th Steklov approximations of the HR Problem on $[-1, 1] \times [-1, 1]$ for $\eta = \eta_2$ corresponding to $M=8$ (Left top), 16(Right top), 48(Left bottom), and 100(Right bottom).

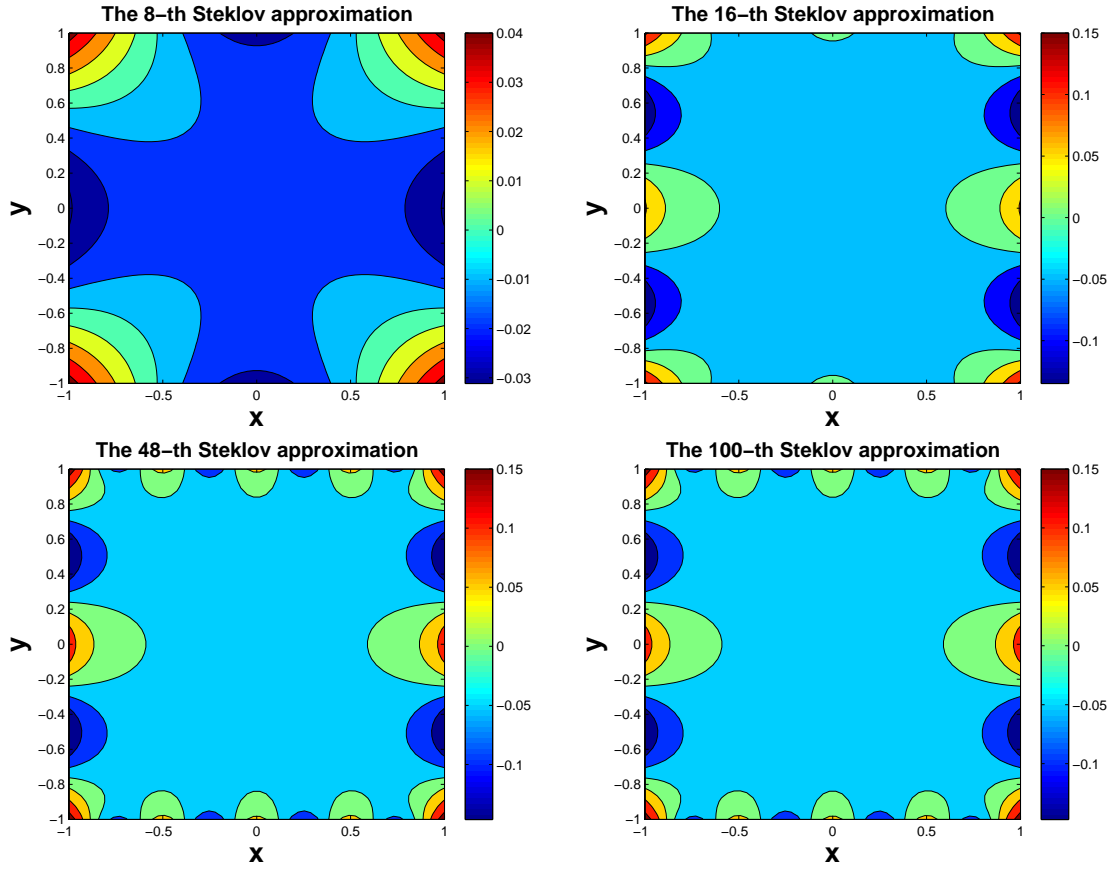


Figure 5.14: Contour lines of the M -th Steklov approximations of the HR Problem on $[-1, 1] \times [-1, 1]$ for $\eta = \eta_3$ corresponding to $M=8$ (Left top), 16(Right top), 48(Left bottom), and 100(Right bottom).

5.4 The Generalized Boundary Data

In this section, we generalize the boundary conditions. Consider finding a solution $u \in H^1(\Omega)$ satisfies that for $t \in [0, 1)$,

$$\Delta u = 0 \quad \text{in } \Omega \quad (5.17)$$

$$(1-t)D_\nu u + tu = \eta \quad \text{on } \partial\Omega \quad (5.18)$$

Here $\eta \in L^2(\partial\Omega, d\sigma)$. Taking $t = 0$ in (5.18) provides the Neumann boundary condition. The Dirichlet problem can be treated as the limit $t \rightarrow 1^-$ of the above problem.

For $0 < t < 1$, we again represent a solution of this problem by $u(x, y) = \sum_{i=0}^{\infty} c_i \hat{s}_i(x, y)$ on Ω for non zero constant c_i , $i \geq 0$. Then the boundary condition yields that

$$\begin{aligned} (1-t)D_\nu u(x, y) + tu(x, y) &= (1-t) \sum_{i=0}^{\infty} c_i D_\nu \hat{s}_i(x, y) + t \sum_{i=0}^{\infty} c_i \hat{s}_i(x, y) \\ &= (1-t) \sum_{i=0}^{\infty} c_i \delta_i \hat{s}_i(x, y) + t \sum_{i=0}^{\infty} c_i \hat{s}_i(x, y) \\ &= \sum_{i=0}^{\infty} ((1-t)\delta_i + t) c_i \hat{s}_i(x, y) \end{aligned}$$

Then (5.9) implies that

$$c_i = \frac{\langle \eta, s_j \rangle_{2, \partial\Omega}}{(1-t)\delta_j + t} \quad \text{for } i \geq 0 \quad (5.19)$$

Theorem 9.2 of [1] says that this problem has a unique solution. Hence the unique

5.4 THE GENERALIZED BOUNDARY DATA

solution u of (5.17)-(5.17) has the Steklov series representation

$$u(x, y) = \sum_{i=0}^{\infty} \frac{\langle \eta, s_j \rangle_{2, \partial\Omega}}{(1-t)\delta_j + t} \hat{s}_i(x, y) \text{ for } (x, y) \in \bar{\Omega} \quad (5.20)$$

for $0 < t < 1$.

Chapter 6

An Application of the Steklov Expansion

6.1 The Mean Value Property

We develop and describe an application of the Steklov expansion of harmonic functions. The Steklov expansion method, to approximate a solution of the certain problem, enables to describe a solution on $\partial\Omega$, but also in $\bar{\Omega}$. In numerical results in the preceding chapter, we saw that the Steklov approximation is flat around the center. We shall investigate to describe solutions of boundary value problems in Ω more precisely.

The *mean value property* provides a way to estimate the value of solutions at the center of Ω . Let u be a harmonic function in a disk D and continuous in its closure \bar{D} . Then the mean value property states that the value of u at the center of D equals the average of u on its circumference(see Section 2.2 of [15]). Note that the mean value property holds where Ω is a disk. Since in this work, Ω is a rectangle, the mean

6.1 THE MEAN VALUE PROPERTY

value property does not always hold.

Now consider the HD problem on $\Omega = [-1, 1] \times [-1, 1]$. We want to find the general formula for $u(0, 0)$ where u is the unique solution of this problem. (5.3) yields that

$$u(0, 0) = \sum_{i=0}^{\infty} \langle \eta, \hat{s}_i \rangle_{2, \partial\Omega} \hat{s}_i(0, 0) \quad (6.1)$$

$$= \langle \eta, \hat{s}_0 \rangle_{2, \partial\Omega} \hat{s}_0(0, 0) + \sum_{i=1}^{\infty} \langle \eta, \hat{s}_i \rangle_{2, \partial\Omega} \hat{s}_i(0, 0) \quad (6.2)$$

$$= \bar{\eta} + \sum_{i=1}^{\infty} \langle \eta, \hat{s}_i \rangle_{2, \partial\Omega} \hat{s}_i(0, 0) \quad (6.3)$$

$$= \bar{\eta} + \sum_{k \in K} \langle \eta, \hat{s}_k \rangle_{2, \partial\Omega} \hat{s}_k(0, 0) \quad (6.4)$$

Here $\{\hat{s}_k : k \in K\}$ is the subset of \mathcal{S} such that $\hat{s}_k(0, 0) \neq 0$ for $k \geq 1$. These results may be summarized as follows.

Theorem 6.1. *Assume Ω , $\partial\Omega$, \mathcal{S} , δ_i , and \hat{s}_i are defined in Chapter 3 and the set K is defined as above. Also assume that u is a harmonic function on Ω with $u = \eta$ on $\partial\Omega$. Then $u(0, 0)$ is given by (6.4).*

In particular the "correction term" to the mean value theorem is $C := \sum_{k \in K} \langle \eta, \hat{s}_k \rangle_{2, \partial\Omega} \hat{s}_k(0, 0)$. This is the difference between $u(0, 0)$ and the mean value of u on $\partial\Omega$.

Here we shall describe the set K in (6.4). Since $\sin(0) = \sinh(0) = 0$, $s_i(0, 0) = 0$ for most i . Only the cch and chc Steklov eigenfunctions are non-zero at the center. So K is the set of orders of cch and chc Steklov eigenfunctions and given by

$$K = \{4, 5, 12, 13, 20, 21, 28, 29, 36, 37, 44, 45, 54, 55, \dots\} \quad (6.5)$$

6.1 THE MEAN VALUE PROPERTY

We list \hat{s}_k for $4 \leq k \leq 95$.

$$\hat{s}_4 = 0.36926 \cos(2.365x) \cosh(2.365y)$$

$$\hat{s}_5 = 0.36926 \cosh(2.365x) \cos(2.365y)$$

$$\hat{s}_{12} = 0.016382 \cos(5.4978x) \cosh(5.4978y)$$

$$\hat{s}_{13} = 0.016382 \cosh(5.4978x) \cos(5.4978y)$$

$$\hat{s}_{20} = 7.0799e^{-4} \cos(8.6394x) \cosh(8.6394y)$$

$$\hat{s}_{21} = 7.0799e^{-4} \cosh(8.6394x) \cos(8.6394y)$$

$$\hat{s}_{28} = 3.0595e^{-5} \cos(11.781x) \cosh(11.781y)$$

$$\hat{s}_{29} = 3.0595e^{-5} \cosh(11.781x) \cos(11.781y)$$

$$\hat{s}_{36} = 1.3221e^{-6} \cos(14.923x) \cosh(14.923y)$$

$$\hat{s}_{37} = 1.3221e^{-6} \cosh(14.923x) \cos(14.923y)$$

$$\hat{s}_{44} = 5.7134e^{-8} \cos(18.064x) \cosh(18.064y)$$

$$\hat{s}_{45} = 5.7134e^{-8} \cosh(18.064x) \cos(18.064y)$$

$$\hat{s}_{54} = 2.469e^{-9} \cos(21.206x) \cosh(21.206y)$$

$$\hat{s}_{55} = 2.469e^{-9} \cosh(21.206x) \cos(21.206y)$$

$$\hat{s}_{62} = 1.0669e^{-10} \cos(24.347x) \cosh(24.347y)$$

$$\hat{s}_{63} = 1.0669e^{-10} \cosh(24.347x) \cos(24.347y)$$

$$\hat{s}_{70} = 4.6107e^{-12} \cos(27.489x) \cosh(27.489y)$$

$$\hat{s}_{71} = 4.6107e^{-12} \cosh(27.489x) \cos(27.489y)$$

$$\hat{s}_{78} = 1.9925e^{-13} \cos(30.631x) \cosh(30.631y)$$

$$\hat{s}_{79} = 1.9925e^{-13} \cosh(30.631x) \cos(30.631y)$$

6.1 THE MEAN VALUE PROPERTY

$$\hat{s}_{86} = 8.6102e^{-15} \cos(33.772x) \cosh(33.772y)$$

$$\hat{s}_{87} = 8.6102e^{-15} \cosh(33.772x) \cos(33.772y)$$

$$\hat{s}_{94} = 3.7208e^{-16} \cos(36.914x) \cosh(36.914y)$$

$$\hat{s}_{95} = 3.7208e^{-16} \cosh(36.914x) \cos(36.914y)$$

We note that $\max_{(x,y) \in \partial\Omega} \hat{s}_k = 1.9826$ for $k=4$ and 5 , $\max_{(x,y) \in \partial\Omega} \hat{s}_k = 2$ for $12 \leq k \leq 95$ when evaluated to 4 decimal places.

k	4	5	12	13	20	21
$\hat{s}_k(0,0)$	0.36926	0.36926	0.016382	0.016382	$7.0799e^{-4}$	$7.0799e^{-4}$
k	28	29	36	37	44	45
$\hat{s}_k(0,0)$	$3.0595e^{-5}$	$3.0595e^{-5}$	$1.3221e^{-6}$	$1.3221e^{-6}$	$5.7134e^{-8}$	$5.7134e^{-8}$
k	54	55	62	63	70	71
$\hat{s}_k(0,0)$	$2.469e^{-9}$	$2.469e^{-9}$	$1.0669e^{-10}$	$1.0669e^{-10}$	$4.6107e^{-12}$	$4.6107e^{-12}$
k	78	79	86	87	94	95
$\hat{s}_k(0,0)$	$1.9925e^{-13}$	$1.9925e^{-13}$	$8.6102e^{-15}$	$8.6102e^{-15}$	$3.7208e^{-16}$	$3.7208e^{-16}$

Table 6.1: $\hat{s}_k(0,0)$

In Table (6.1), we report $\hat{s}_k(0,0)$ for $4 \leq k \leq 95$ and it corresponds to $\|s_k\|_{2,\partial\Omega}^{-1}$ where s_k is the Steklov eigenfunction defined in Section 3.5. For $4 \leq k \leq 95$, $\hat{s}_k(0,0)$ is decreasing and getting closer to 0 against k .

Now we are concerned with how these values are decreasing. Let k_r be the r -th element of the set K . In other words, r represents an index of k in the set K . Here we suspect that the graph of $\hat{s}_{k_r}(0,0)$ against r is the exponential decay like e^{-ar} for non zero constant a . Then

$$\log(|\hat{s}_{k_{r+2}}(0,0) - \hat{s}_{k_r}(0,0)|) = \log(|e^{-a(r+2)} - e^{-ar}|) \quad (6.6)$$

6.1 THE MEAN VALUE PROPERTY

$$= \log(|e^{-ar} \cdot (e^{-2a} - 1)|) \quad (6.7)$$

$$= -ar + C \quad (6.8)$$

where $C := \log(|e^{-2a} - 1|)$. In Figure (6.1), we observe that $\log(|\hat{s}_{k_{r+2}}(0, 0) - \hat{s}_{k_r}(0, 0)|)$ is the decay linearly against r .

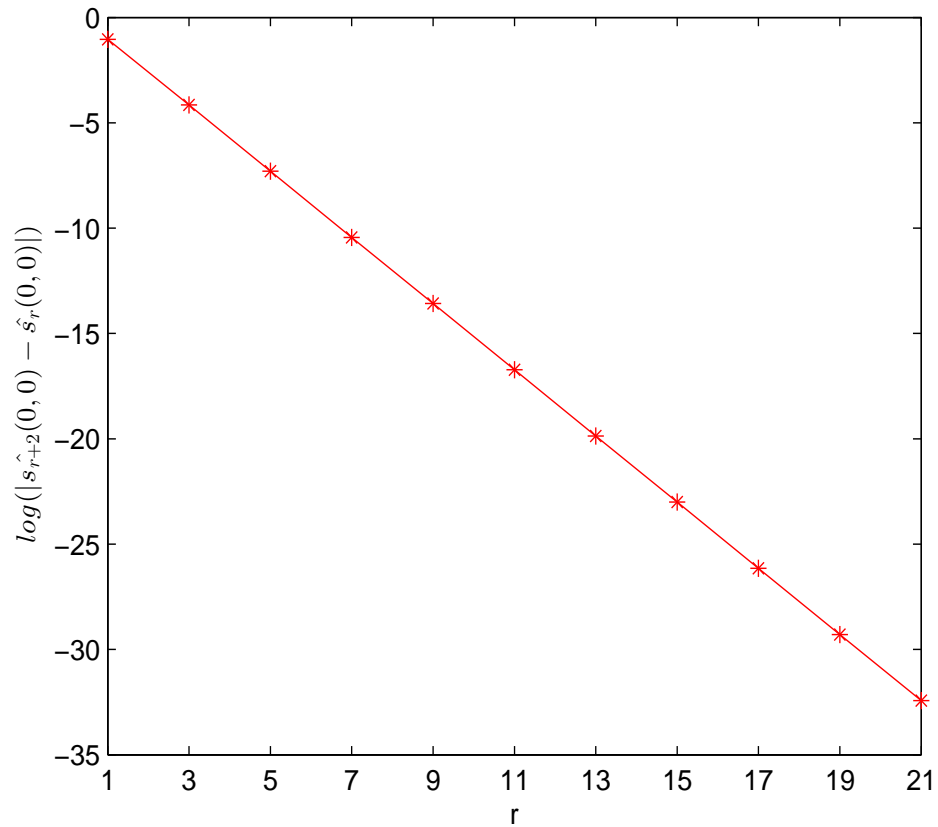


Figure 6.1: The linear decay of $\log(|\hat{s}_{k_{r+2}}(0, 0) - \hat{s}_{k_r}(0, 0)|)$ with the approximated slope, -1.5694 for $1 \leq r \leq 21$.

6.2 The Correction Term

Let $K_r = \{k_i \mid 1 \leq i \leq r\}$. Define $CD(r) := \sum_{k \in K_r} \langle \eta, \hat{s}_k \rangle_{2, \partial\Omega} \hat{s}_k(0, 0)$ to be the r -th correction term of $u(0, 0)$ where u is a solution of the HD problem with $\eta = \Gamma u$. In this section, we shall describe this correction term. Completeness of the Steklov expansion of the solution of the HD problem ensures that $\lim_{r \rightarrow \infty} CD(r) = u(0, 0) - \bar{\eta}$. We are concerned with the number of the Steklov eigenfunctions in the correct term required to converge to a certain accuracy.

We recall $u_1(x, y) = x^2 - y^2$, $u_2(x, y) = x^3 - 3xy^2$, and $u_3(x, y) = e^x \cos(y)$ from Section 4.2. Let $\eta_i = \Gamma u_i$ for $1 \leq i \leq 3$. These functions are H^1 -harmonic functions on Ω and their traces are continuous on the boundary. We know that $\bar{\eta}_1 = \bar{\eta}_2 = 0$ and $\bar{\eta}_3 = 0.96671$. Also we notice that $u_1(0, 0) = u_2(0, 0) = 0$ and $u_3(0, 0) = 1$. Denote the r -th the correction term of $u_i(0, 0)$ by $CD_i(r)$ for $1 \leq i \leq 3$. Then we suspect that when $i = 1$ and $i = 2$, $CD_i(r) \rightarrow 0$ as $r \rightarrow \infty$ and when $i = 3$, $CD_3(r) \rightarrow 0.03329$ as $r \rightarrow \infty$.

We notice that when η is odd about the center on each side of the boundary then $\langle \eta, \hat{s}_k \rangle_{2, \partial\Omega} = 0$ for all $k \in K$. It implies that $\langle \eta_2, \hat{s}_k \rangle_{2, \partial\Omega} = 0$ for all $k \in K$ so that $CD_2(r) = 0$ for all r . In this case, there is no difference between $u_2(0, 0)$ and its mean value on the boundary. Here we can see how much the Steklov expansion of harmonic functions is efficient.

Numerical experiments of approximations of $u_1(0, 0)$ are reported in Table (6.2) and it shows that the 21th correction term of $u_1(0, 0)$ gives a nice approximation of $u_1(0, 0)$.

For u_3 , we evaluate $(u_3(0, 0) - \bar{u}_3) - CD_3(r)$ to see how it decreases to zero. Table (6.3) shows that the 21th correction term of $u_3(0, 0)$ can be a good approximation of

6.2 THE CORRECTION TERM

r	7	9	11	13
$CD_1(r)$	$6.2349e^{-7}$	$-1.6793e^{-8}$	$4.9523e^{-10}$	$-1.5529e^{-11}$
r	15	17	19	21
$CD_1(r)$	$5.0908e^{-13}$	$-1.7258e^{-14}$	$6.0066e^{-16}$	$-2.1352e^{-17}$

Table 6.2: The r-th correction term of u_1

$u_3(0, 0) - \bar{u}_3$. We again suspect that the graph of the r-th correction term against r is

r	7	9	11	13
$(u_3(0, 0) - \bar{u}_3) - CD_3(r)$	$-3.0348e^{-7}$	$8.1522e^{-9}$	$-2.4008e^{-10}$	$7.5188e^{-12}$
r	15	17	19	21
$(u_3(0, 0) - \bar{u}_3) - CD_3(r)$	$1.3451e^{-13}$	$-1.2321e^{-14}$	$7.2873e^{-16}$	$2.3984e^{-18}$

Table 6.3: The difference between $CD_3(r)$ and $(u_3(0, 0) - \bar{u}_3)$

the exponential decay as described in the previous chapter. Then we consider the linear graph of $\log(|CD_i(r+2) - CD_i(r)|)$ against r to estimate of the rate of convergence for the approximations as a function of r. In Figure (6.2), we can observe how fast each correction term converges by using only 24 cch and chc Steklov eigenfunctions. These results show that only a few terms in the Steklov expansion are necessary to obtain good approximations of the value of the solution of the HD problem at the center of Ω .

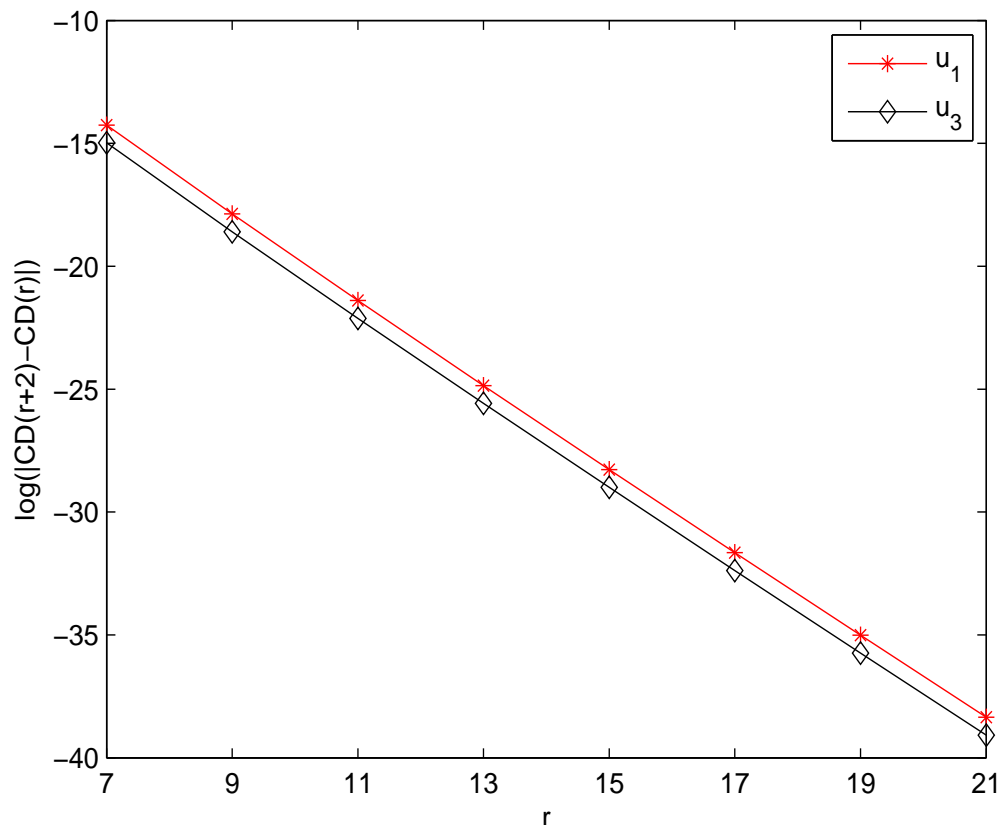


Figure 6.2: The linear decay of $\log(|CD_1(r+2) - CD_1(r)|)$ and $\log(|CD_3(r+2) - CD_3(r)|)$ with their approximated slopes, -1.7206 and -1.721 , respectively.

6.3 Several Examples

In this section, we develop the formulae of $u(0,0)$ where $u(x,y)$ are solutions of Laplace's equation subject to certain boundary condition on Ω . We consider the problem of finding non trivial solutions in $H^1(\Omega)$ that satisfy

$$\Delta u = 0 \quad \text{in } \Omega \quad (6.9)$$

$$D_\nu u + bu = \eta \quad \text{on } \partial\Omega \quad (6.10)$$

6.3 SEVERAL EXAMPLES

where b is a constant. Here $\eta \in L^2(\partial\Omega, d\sigma)$. Then (6.10) will be treated as the Neumann boundary condition when $b=0$ or the Robin boundary condition when $b=1$.

When $b \neq 0$, from the analysis of the previous chapter the unique solution of this problem has the Steklov series representation

$$u(x, y) = \sum_{i=0}^{\infty} \frac{\langle \eta, \hat{s}_i \rangle_{2, \partial\Omega}}{b + \delta_i} \hat{s}_i(x, y) \text{ for } (x, y) \in \bar{\Omega} \quad (6.11)$$

Then the explicit formula of $u(0, 0)$ is given by

$$u(0, 0) = \frac{\bar{\eta}}{b} + \sum_{k \in K} \frac{\langle \eta, \hat{s}_k \rangle_{2, \partial\Omega}}{b + \delta_k} \hat{s}_k(0, 0) \quad (6.12)$$

Here the set K is defined in (6.5).

When $b = 0$ and $\bar{\eta} = 0$, (5.12) yields that

$$u(0, 0) = \sum_{k \in K} \frac{\langle \eta, \hat{s}_k \rangle_{2, \partial\Omega}}{\delta_k} \hat{s}_k(0, 0) \quad (6.13)$$

Define $CN(r) := \sum_{k \in K_r} \frac{\langle \eta, \hat{s}_k \rangle_{2, \partial\Omega}}{\delta_k} \hat{s}_k(0, 0)$ to be the r -th correction term of $u(0, 0)$ where u is a solution of the HN problem. Also we define $CR(r) := \sum_{k \in K_r} \frac{\langle \eta, \hat{s}_k \rangle_{2, \partial\Omega}}{1 + \delta_k} \hat{s}_k(0, 0)$ to be the r -th correction term of $u(0, 0)$ where u is a solution of the HR problem.

Now we have the machinery to perform numerical experiments which show that the value of solutions at the center can be nicely approximated by our formulae.

Let $\Omega = [-1, 1] \times [-1, 1]$. Denote the solution of the HD, HN, and HR problem on Ω by u_D , u_N , and u_R , respectively. We recall η_1 , η_2 , and η_3 from Section 5.1. We note that $\bar{\eta}_1 = \frac{2}{3}$, $\bar{\eta}_2 = 1$, and $\bar{\eta}_3 = 0$.

6.3 SEVERAL EXAMPLES

Since η_2 is odd about the center on each side of the boundary, then $\langle \eta_2, \hat{s}_k \rangle_{2, \partial\Omega} = 0$ for all $k \in K$. Then $u_D(0, 0) = u_R(0, 0) = \bar{\eta}_2 = 1$. In other words, the value of each solution at the center of Ω is exactly obtained by the mean value of each solution on the boundary.

Next we let $\eta = \eta_1$. In this case, there is no solution of the HN problem since $\bar{\eta}_1 \neq 0$. We evaluate the r -th correction terms of $u_D(0, 0)$ and $u_R(0, 0)$, respectively. Table (6.4) reports absolute values of the difference between the r -th and the $(r+2)$ -th correction terms corresponding to $u_D(0, 0)$ and $u_R(0, 0)$, respectively. These results show that $u_D(0, 0) \approx \bar{\eta}_1 + CD(23) = 0.66667 + 0.15459 = 0.82126$ and $u_R(0, 0) \approx \bar{\eta}_1 + CR(23) = 0.66667 + 0.046594 = 0.71326$. In Figure (6.3), we observe how fast each correction term converges within $r=23$ and the bounded error of each correction term is quite small.

r	7	9	11	13
$ CD(r+2) - CD(r) $	$3.1164e^{-7}$	$8.3923e^{-9}$	$2.476e^{-10}$	$7.7686e^{-12}$
r	15	17	19	21
$ CD(r+2) - CD(r) $	$2.5481e^{-13}$	$8.6429e^{-15}$	$3.0095e^{-16}$	$1.0703e^{-17}$
r	7	9	11	13
$ CR(r+2) - CR(r) $	$2.4258e^{-8}$	$5.246e^{-10}$	$1.2932e^{-11}$	$3.4848e^{-13}$
r	15	17	19	21
$ CR(r+2) - CR(r) $	$1.0017e^{-14}$	$3.0237e^{-16}$	$9.4852e^{-18}$	$3.0691e^{-19}$

Table 6.4: Absolute values of the difference of the r -th and the $(r+2)$ -th correction terms for $\eta = \eta_1$ corresponding to $u_D(0, 0)$ and $u_R(0, 0)$, respectively

Now we let $\eta = \eta_3$. We perform similar experiments and results are given in Table (6.5) and Figure (6.4). Figure (6.4) shows that each correction term converges quickly. Then $u_D(0, 0) \approx CD(23) = -0.030398$, $u_N(0, 0) \approx CN(23) = -0.015236$, and $u_R(0, 0) \approx CR(23) = -0.010421$.

Here we emphasize that only a few Steklov eigenfunctions are required to approx-

6.3 SEVERAL EXAMPLES

r	7	9	11	13
$ CD(r+2) - CD(r) $	$1.5451e^{-6}$	$3.7155e^{-8}$	$9.8596e^{-10}$	$2.8002e^{-11}$
r	15	17	19	21
$ CD(r+2) - CD(r) $	$8.3568e^{-13}$	$2.5923e^{-14}$	$8.2967e^{-16}$	$2.7253e^{-17}$
r	7	9	11	13
$ CN(r+2) - CN(r) $	$1.3405e^{-7}$	$2.5171e^{-9}$	$5.5001e^{-11}$	$1.3285e^{-12}$
r	15	17	19	21
$ CN(r+2) - CN(r) $	$3.4498e^{-14}$	$9.4718e^{-16}$	$2.7193e^{-17}$	$8.0983e^{-19}$
r	7	9	11	13
$ CR(r+2) - CR(r) $	$1.234e^{-7}$	$2.3577e^{-9}$	$5.2098e^{-11}$	$1.2684e^{-12}$
r	15	17	19	21
$ CR(r+2) - CR(r) $	$3.3131e^{-14}$	$9.1381e^{-16}$	$2.633e^{-17}$	$7.8647e^{-19}$

Table 6.5: Absolute values of the difference of the r -th and the $(r+2)$ -th correction term for $\eta = \eta_3$ corresponding to $u_D(0, 0)$, $u_N(0, 0)$, and $u_R(0, 0)$, respectively

imate the value of solutions at the center of Ω with a high accuracy. Moreover, when η is odd about the center on each side of the boundary, then $u_D(0, 0)$, $u_N(0, 0)$ (if $\bar{\eta} = 0$), and $u_R(0, 0)$ are exactly computed and the values equal $\bar{\eta}$.

6.3 SEVERAL EXAMPLES

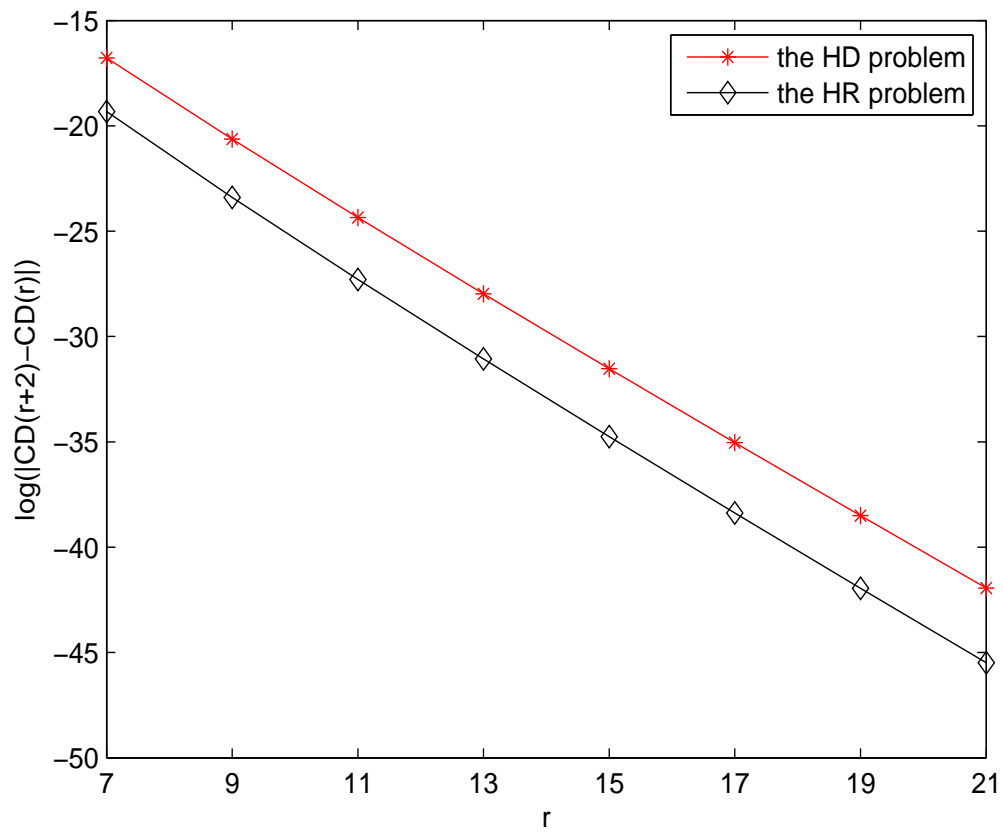


Figure 6.3: The linear decay of $\log(|CD(r+2) - CD(r)|)$ and $\log(|CR(r+2) - CR(r)|)$ with their approximated slopes, -1.7973 and -1.8689, respectively.

6.3 SEVERAL EXAMPLES

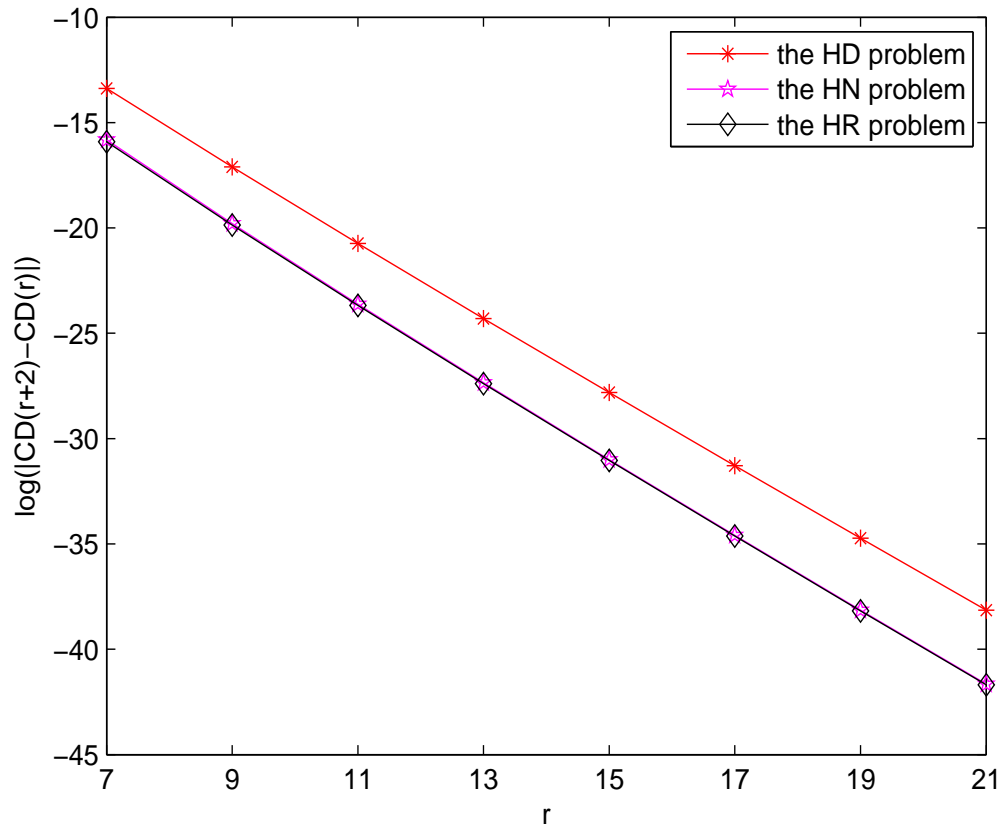


Figure 6.4: The linear decay of $\log(|CD(r+2) - CD(r)|)$, $\log(|CN(r+2) - CN(r)|)$ and $\log(|CR(r+2) - CR(r)|)$ with their approximated slopes, -1.7686, -1.8452, and -1.8412, respectively.

Bibliography

- [1] G. Auchmuty. *Steklov eigenproblems and the representation of solutions of elliptic boundary value problems*. Numer. Funct. Anal. Optim. **25** (2004), 321-348.
- [2] G. Auchmuty. *Spectral characterizations of the trace spaces $H^s(\partial\Omega)$* . SIAM J. Math. Anal. **38** (2006), 894-905.
- [3] G. Auchmuty and P. Kloucek *Generalized harmonic functions and the dewetting of thin films*. Appl. Math. Optim. **55** (2007), 145-161.
- [4] G. Auchmuty *Reproducing kernels for Hilbert spaces of real harmonic functions*. SIAM J. Math. Anal. **41** (2009), 1994-2009.
- [5] R. A. Adams and J. J. F. Fournier. *Sobolev Spaces*. Second Edition. Elsevier/Academic Press, Amsterdam (2003).
- [6] C. Bandle. *Isoperimetric Inequalities and Applications*. Pitman, London (1980).
- [7] G. Dahlquist and A. Bjorck. *Numerical Methods in Scientific Computing: Volume I*. Society for Industrial and Applied Mathematics, PI (2008).
- [8] E. DiBenedetto. *Real Analysis*. Birkhauser, Boston (2001).
- [9] R. Dautray and J-L. Lions. *Mathematical Analysis and Numerical Methods for Science and Technology*. Vol. 1. Springer-Verlag, Berlin (1990).

BIBLIOGRAPHY

- [10] D. W. Fox and J. R. Kuttler. *Sloshing Frequencies* Z. Angew. Math. Phys. **34** (1983), 668-696.
- [11] P. Grisvard. *Elliptic Problems in Nonsmooth Domains*. Pitman, Boston (1985).
- [12] W. Gander. and W. Gautschi. *Adaptive Quadrature Revisited*. BIT. Vol. 40 (2000), 84-101
- [13] C. Kenig. *Harmonic Analysis Techniques for Second Order Elliptic Boundary Value Problems*. CBMS Reg. Conf. Ser. Math. 83. AMS, Providence, RI (1994).
- [14] P. Kloucek, D. C. Sorensen and J. L. Wightman *The approximation and computation of a basis of the trace space $H^{\frac{1}{2}}$* . J. Sci. Comput. Volume 32, Issue 1, (2007), 73-108.
- [15] L.C. Evans. *Partial Differential Equations*. Second edition. American Mathematical Society, Providence, RI (2010).
- [16] L.C. Evans and R.F. Gariepy. *Measure Theory and Fine Properties of Functions*. CRC Press, Boca Raton, FL (1992).
- [17] J. Necas. *Direct Methods in the Theory of Elliptic Equations*. Springer-Verlag, New York (2012).
- [18] P. McIver. *Sloshing frequencies for cylindrical and spherical containers filled to an arbitrary depth*. Journal of Fluid Mechanics. **201**, 243-257.
- [19] R. C. McOwen. *Partial Differential Equations: Methods and Applications*. Second Edition. Pearson Education Inc., New Jersey (2003).
- [20] W. A. Strauss. *Partial Differential Equations: An Introduction*. Second Edition. John Wiley and Sons Inc., New York (2008).
- [21] E. Zeidler. *Nonlinear Functional Analysis and Its Applications: IIA*. Springer-Verlag, New York (1985).